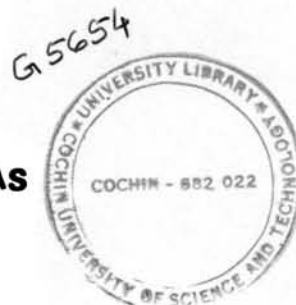# ELECTRO-OPTICAL PROPERTIES OF METAL PHTHALOCYANINES AND NAPHTHALOCYANINES

THESIS SUBMITTED TO
THE COCHIN UNIVERSITY OF SCIENCE AND TECHNOLOGY
IN PARTIAL FULFILMENT OF THE REQUIREMENTS
FOR THE DEGREE OF
DOCTOR OF PHILOSOPHY
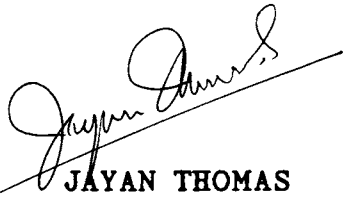IN THE
FACULTY OF SCIENCE

By

JAYAN THOMAS

DEPARTMENT OF APPLIED CHEMISTRY
COCHIN UNIVERSITY OF SCIENCE AND TECHNOLOGY
KOCHI – 682 022, INDIA

DECEMBER 1995

DECLARATION

I hereby declare that the work presented in this thesis is based on the original work done by me under the guidance of Dr. V.N.Sivasankara Pillai, Professor, School of Environmental Studies, Cochin University of Science and Technology, and that no part of this thesis has been included in any other thesis submitted previously for the award of any degree.

Cochin-22,
15 December 1995.

JAYAN THOMAS

Dr.V.N. Sivasankara Pillai

Professor,

School of Environmental Studies,

Cochin University of Science and Technology,

Fine Arts Avenue,

Kochi-682016.

Cochin-16,

15 Decmber 1995

CERTIFICATE

Certified that the work presented in this thesis is based on the bonafide work done by Mr.Jayan Thomas under my guidance in the Department of Applied Chemistry, Cochin University of Science and Technology and that no part thereof has been included in any other thesis submitted previously for the award of any degree.

(V.N. SIVASANKARA PILLAI)

PREFACE

Organic dyes and pigments are routinely used as colouring agents. Many of them also find application in high technology areas like photon harvesting, photodynamic therapy, optical imaging and data recording. Naphthalocyanines and phthalocyanines have been the focus of active research due to their chemical stability, biological tolerance, high light absorptivity, and semiconducting properties. From the point of view of optical imaging and data recording, metal phthalocyanines and naphthalocyanines have moderate processability and low cost. For these applications, a knowledge of their optical, thermal, and electrical properties is a prerequisite.

This dissertation deals with the preparation and chemical, optical, thermal, and electrical characterization of five compounds, namely metal free naphthalocyanine, vanadyl naphthalocyanine, zinc naphthalocyanine, europium dinaphthalocyanine, and europium diphthalocyanine in the pristine and iodine-doped forms. The properties of these materials in the bulk and thin film forms differ, but are amenable to correlation. Due to the simplicity of experimentation, the results reported herein are based on samples in the form of compressed pellets.

Metal phthalocyanines have very similar optical properties. The slight variation in the optical properties can arise from the influence of the central metal atom. However the electrical properties, especially in the doped states may differ considerably due to the variable oxidation states that a metal can assume and due to the degeneracy of the energy states of the oxidised phthalocyanine system and the metal atom. Thus, in the case of nickel phthalocyanine, iodine-doped state acts as a "metal" in terms of its electrical conductivity.

The materials selected in this study have some common features that will help to draw certain logical conclusions. Thus a comparison of the properties of metal free naphthalocyanine and zinc naphthalocyanine shows the influence of the central metal atom on the properties of metal naphthalocyanines. Again, vanadyl naphthalocyanine represents another feature associated with the central metal atom. The interesting property of europium as a central atom is its unique optical properties. Moreover, this is a case where a dinaphthalocyanine is formed.

Except for some preliminary reports on its synthesis and chemical characterization, very little work has been reported on europium dinaphthalocyanine. The work on europium

dinaphthalocyanine reported in this dissertation fills this information lacuna.

The dissertation is broadly divided into six chapters. The first chapter is a brief overview on the present status of work on metal phthalocyanines and naphthalocyanines. Efforts have been made to highlight the recent trends in research on these materials. The second chapter summarizes the experimental methodologies used in the synthesis, purification, and characterization of the target compounds. A brief discussion of the characterization is also included.

Two important technological properties of these compounds have been investigated. The electrical properties are important in applications in sensors and semiconductor lasers. Opto-thermal properties assume significance for optical imaging and data recording. The electrical properties were investigated by dc and ac techniques. DC conductivity was measured with pristine and iodine-doped samples as a function of temperature. The results were complemented by measuring ac conductivity as a function of temperature at selected frequencies. Efforts were made to delineate the conduction mechanism. Details of these studies are presented in chapter III.

Chapter IV and V describe the evaluation of thermal diffusivity of these samples by optical methods. Photoacoustic technique is described in chapter IV. Photothermal deflection method is presented in chapter V. Both the techniques use an intense laser beam as a pump source, but the detection techniques differ. For this reason, the experimental procedures and results are presented in two different chapters.

The last chapter (chapter VI) summarises the salient features of the results obtained in these studies.

CONTENTS

CHAPTER I

METAL PHTHALOCYANINES AND NAPHTHALOCYANINES —

A BRIEF SURVEY

Abstract

Metal phthalocyanines and naphthalocyanines are candidate materials in high technology applications like photodynamic therapy, photovoltaic devices, imaging and information storage. The large volume of work being done recently on these compounds points to their relevance. The status of the work on phthalocyanines and naphthalocyanines are reviewed in this chapter. Due to the very large number of publications appearing recently, the scope of this review was curtailed to highlight only their optical and electrical properties. Important applications are also mentioned briefly.

1.1   INTRODUCTION

Metal phthalocyanines (MPcs) and naphthalocyanines (MNcs) have been of wide interest to the scientific world since their discovery in 1908.[1-3] They are candidate materials for application in colouration, photovoltaic devices, imaging, catalysis, optoelectronics and information storage.[4,5] Most of the properties of phthalocyanines (tetrabenzo[2,3] porphyrazines) and naphthalocyanines (tetranaphtho[2,3] porphyrazines) depend on π-electron conjugation in the macrocyclic ring. They have excellent stability against heat, light, moisture and air.

Of late, MNcs have been the focus of research as materials for high density optical data recording (ODR) media[6-10] due to their excellent chemical stability, low heat conduction and diversity of optical properties. The major advantages of these organic dyes over metallic materials for ODR applications are their amenability for engineering their molecular structure and their processability to be cast as thin films by vacuum sublimation. For writing and reading using semiconductor lasers ODR materials require high optical absorptivity in the longer wavelength region (700–900 nm). Some of the metal phthalocyanines such as MgPc[11] and VOPc[12] are known to exhibit absorption in this wavelength region. The need for longer wavelength absorption systems has led to the synthesis of phthalocyanines with engineered molecular structure.

Naphthalocyanines have strong absorption bands in the near infrared region because of their extended π-electron conjugated systems with the additional benzoannulation.[13,14] Long wavelength absorption and stable planar molecular structure together with their ability to be cast into thin films make MNcs one of the most competitive candidates for ODR media.[15,16]

Solar energy conversion is a promising technology since it is environment friendly and inexhaustible. Eventhough some of the inorganic semiconductors like silicon have energy conversion efficiency greater than 10%,[17] the electrical energy obtained with these cells is expensive. On the other hand organic semiconductors are promising materials for future solar energy conversions because of the low processing cost of organic thin films and nearly unlimited variability.[18] The solar energy conversion system in nature namely, photosynthesis, functions with chlorophyll in which the ligand, porphyrin is structurally analogous to MNc and MPc ring systems, synthetic organic molecules could be tailored to mimic the natural system.

In addition to the very interesting optical properties of MNcs and MPcs, they show attractive electrical properties which find application in semiconductor devices.[19,20] The electrical conductivity of these materials can be easily amended by doping with suitable dopants.[21]
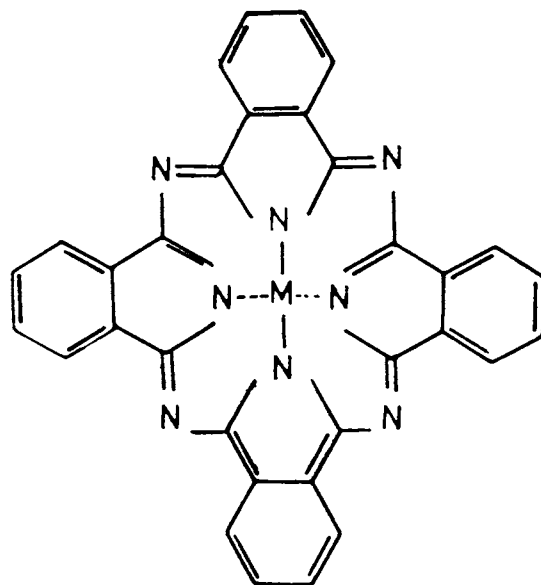
Figure 1.1a   Structure of metal phthalocyanine

Phthalocyanines   and   naphthalocyanines   are   structural analogues of porphyrines. The inner ring system of Pcs and Ncs is made up of pyrrole rings joined together by aza (-N=) groups. A benzene ring is attached to the β position of each of the pyrrole groups to form a phthalocyanine molecule and a naphthalene ring attached to the β position forms a naphthalocyanine molecule.

4
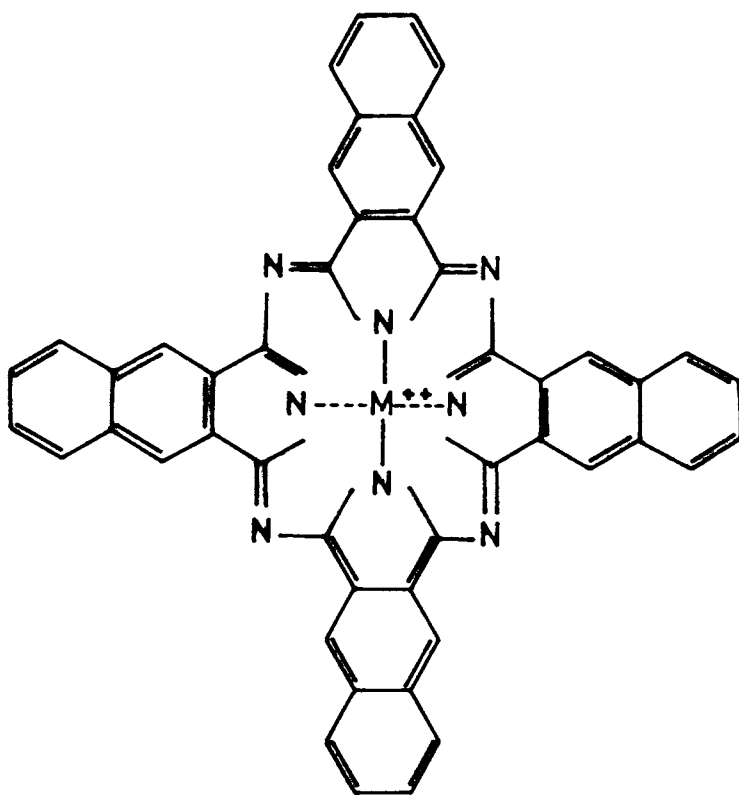
Figure 1.1 b   Structure of Metal naphthalocyanine

groups to form a phthalocyanine molecule and a naphthalene ring attached to the β position forms a naphthalocyanine molecule.

In MPcs and MNcs, the central atom displaces two hydrogen ions from the isoindole group and practically finds itself in a symmetrical electrostatic field of four nitrogen atoms with which it may form four equivalent or almost equivalent coordinate donor-acceptor bonds (Figure 1.1 a and b). The central atom can be any of the metal atoms in the periodic table. In order to get a variety of MPc and MNc derivatives the sixteen peripheral hydrogen atoms on the benzene rings are replaced with suitable atoms and groups.

The structural diversity of porphyrins, phthalocyanines and naphthalocyanines is the main factor responsible for their importance in various physicochemical and biological studies. This structural diversity opens up unlimited possibilities for studying the effect of functional substituents and central atoms on the properties of these compounds. Such studies will enable us to provide an answer to the question why nature was choosy to evolve the porphyrins, chlorophyll and blood as the basic component of life.

1.3   SYNTHESIS OF PHTHALOCYANINES

Metal phthalocyanines are synthesised from structural units making up the macrocyclic ring in presence of the respective metal atom. The widely used method of synthesis is one which is described by Linstead *et al.*[22-25]

1.3.1 Synthesis of rare earth diphthalocyanines

The phthalocyanine complexes of various rare earth elements were synthesised according to the method of Kirin *et al.*[26] In the method described, a mixture of phthalonitrile (8 mmol) and rare earth acetate (1 mmol) was heated in a sealed tube at 290 $^{\circ}$C for 2 h. The compounds were purified by soxhlet extraction using dichloromethane solvent. Further purification was accomplished by dissolving the solid mass in DMF and chromatographing on alumina using methanol or saturated solution of NH_4Cl in 1:2 benzene/methanol mixture as eluent. Very pure samples of rare earth diphthalocyanines have been prepared by direct vacuum sublimation of the samples on glass slides.[27]

Sadak *et al*[28] have confirmed by elemental analysis the presence of two phthalocyanine ligands in the complex. They have

proposed the formula $M(Pc)_2$ for the rare earth diphthalocyanine complexes.

1.4. SYNTHESIS OF NAPHTHALOCYANINES

According to Lukyanets *et al* [29] naphthalocyanines can be prepared by heating respective metal salts with 2,3-dicyanonaphthalene in the stoichiometric ratio 1:4 in presence of ammonium molybdate *at* 260–270 ^{O}C for 5–6 h. Metal naphthalocyanines of Cu, Mg, Zn, Al, Ga, Sn, VO, Mn, Fe, Co, Ni, and Pd were synthesised by this method.[30,31]

The reaction is usually carried out in an evacuated sealed glass ampoule and in some cases under nitrogen atmosphere. Table 1. presents a summary of reaction conditions which have been reported.

Table 1. Reaction conditions for the preparation of 2,3-naphthalocyanines.[19]

Metal or compound	Naphthalocya-nine formed	Temp °C	Time (min.)	Ampoule pressure (Torr)
Copper-Bronze	CuNc	260-270	60	0.02
PbO	PbNc	275	30	0.02
V_2O_5	VONc	280	30	$760(N_2)$
Mg	MgNc	370	80	0.02

1.5. PURIFICATION OF METAL PHTHALOCYANINES AND NAPHTHALOCYANINES

Earlier reports point to the difficulty of purifying metal phthalocyanines.[32] Phthalocyanines prepared by various methods may

be contaminated with unreacted materials such as phthalic anhydride, urea, phthalimide or phthalonitrile. It may also contain a number of oligomers. Purification procedures involved are acid and alkali washing, solvent washing , soxhlet extraction, regeneration by concentrated H_2SO_4, chromatography and vacuum sublimation.

Vacuum sublimation is the most facile method for purifying metal phthalocyanines. Dent *et al* [32] have reported that phthalocyanines sublime under vacuum slowly at 550 ^{O}C and rapidly at 580 ^{O}C. Thin films and very pure crystals of phthalocyanines were prepared by this method.

Chemical purification method involves washing with 10% caustic soda, 2 M HCl, methanol and benzene respectively. The solid mass so obtained is slurried in concentrated sulfuric acid, filtered and dropped over ice. The precipitated phthalocyanine, which may contain various oligomers, is washed with water and dried. It is then soxhlet extracted with acetone, benzene or a suitable solvent.

The rare earth phthalocyanines are usually purified by chromatography. After washing with dilute acid and alkali, rare earth phthalocyanines are dissolved in DMF and passed over a column of aluminium oxide. Methanol is used as the eluent. A saturated

solution of NH_4Cl in 1:2 benzene–methanol mixture can also be used for eluting the separated phthalocyanines. Sadak *et al* [28] have purified Lu, Yb, Er, Dy, Gd, Eu, Nd, La diphthalocyanines by soxhlet extraction using dichloromethane. The solvent extraction method was used by Walton *et al* [33] for the purification of Lu and Yb diphthalocyanine. The required product was isolated from the reaction mixture by extraction with chloroform. Evaporation of the solvent gave a green powder which was carefully washed with organic solvents like acetic anhydride, methanol and acetone.

According to Kaplan *et al* [19] naphthalocyanines formed from 2,3-dicyanonaphthalene yield only a single isomer whereas one formed from 1,2-dicyanonaphthalene is a mixture of several structural isomers that were difficult to separate and characterize. Purification of 2,3-naphthalocyanine was accomplished by exhaustive washing with halogenated hydrocarbon solvents or sublimation of the more volatile impurities in vacuum. Cu, Pb, VO and Mg naphthalocyanines were purified by this method.

1.6   POLYMORPHISM

Three polymorphic forms of phthalocyanines are known from the X-ray diffraction studies.[34-36] They are designated by α, β and γ. Monocrystals of phthalocyanines in most cases are of the β type.

They are generally grown by sublimation under a stream of nitrogen at a temperature of 400–500 $^{\circ}$C.

Metal phthalocyanines form polycrystalline films of the α type when evaporated under vacuum ($10^{-5} - 10^{-6}$ Torr) onto a substrate maintained at room temperature. For example the crystallization of CuPc to the α form occurs between 50 and 140 $^{\circ}$C and this phase is stable upto 207 $^{\circ}$C where β form is formed. The α crystalline form is directly obtained if the metal phthalocyanine is sublimed at a pressure less than 50 Torr onto a substrate held at room temperature.

Both solvent and melt methods of synthesis results in the α form of metal phthalocyanine. Heating to 200 $^{\circ}$C reconverts α form to β form. The β form can revert to the α form by dissolution in concentrated sulfuric acid followed by precipitation with water.

The third polymorph γ–CuPc was first reported by Easter.[37] It is obtained by stirring crude CuPc with sulfuric acid of less than 60% concentration. Salts of CuPc made by slurrying in nitrobenzene and adding to a non–oxidising mineral acid followed by filtration and hydrolysis of the filtered salts produces the γ type crystal.

The crystal structure of naphthalocyanines in solid films has

not been determined in detail so far. An expected phase transition in the crystalline film of naphthalocyanines has attracted much interest for application to ODR material.[16] The problem of the presence of various polymorphs of the naphthalocyanines must await careful single crystal X-ray crystallographic analysis.

1.7   SPECTRAL CHARACTERISTICS

In metal phthalocyanines, σ coordination of nitrogen lone pair directed towards centre of the ring occurs with the central metal atoms to form in-plane σ orbitals. Interaction of the metal orbitals with nitrogen $p\pi$ orbitals gives rise to perpendicular-to-the-plane overlaps. The macrocyclic ligands is clearly a donor of electrons to the metal. The π orbitals of the ligands may act both as π donor or acceptor.

The absorption spectra of the metal phthalocyanines are composed of two very intense bands in the 300-400 nm region (Soret band) and in the 650-700 nm region (Q band).

In metal naphthalocyanines, the K band occurs at about 80-100 nm on the higher wavelength side than that of the corresponding phthalocyanine compounds.[38,39] This can be explained by the increased π-electron conjugation the naphthalocyanine ring. Sublimed thin films of H_2Nc, and CuNc show absorption bands at 800 and 785 nm respectively whereas the corresponding phthalocyanine

13

H_2Pc has bands at 700 and 635 nm and CuPc has absorption maxima at 691, 680 and 626 (sh) nm.

Table 2. Absorption maxima of evaporated thin films of various 2,3-naphthalocyanines and metal free phthalocyanines.[19]

Compound	Colour	λ_{max} (nm)	Absorptivity
CuNc	green	712, sh785	1.1×10^5
VONc	green	846, sh 770	4.3×10^5
PbNc	green	846, sh 770	9.8×10^4
MgNc	green	720, sh 788	1.3×10^5
H_2Nc	green	715, sh 800	3.1×10^4
H_2Pc	blue	685, sh700	2.4×10^4

The λ_{max} of naphthalocyanines in the solution phase is less than that of thin films.[40]

14

Infrared spectra of naphthalocyanine samples recorded in CsI pellets show a very strong absorption line at 1085-1081 cm^{-1} which may be attributed to ring breathing modes in the phthalocyanine portion of the molecules. Other prominent peaks are the strong multiplets at 1360 cm^{-1}, the doublet centered near 875 cm^{-1} and 730 cm^{-1} respectively and the singlet at 470 cm^{-1}.

1.8   ELECTRICAL CHARACTERISTICS

The electrical conduction in phthalocyanines has been extensively studied.[41,42] Phthalocyanines and naphthalocyanines are intrinsic semiconductors and the current carriers are mobile π electrons. The temperature dependence of conductivity follows the Arrhenius relation

$$\sigma = \sigma_o \exp (-Ea/2kT)$$

where σ = specific conductivity at temperature T in S cm^{-1}

σ_o = specific conductivity at infinite temperature

Ea = activation energy

k = Boltzman constant

The activation energy Ea represents the energy needed to

liberate charge carriers from traps or to ionize levels within the band gap. The electrical conductivity of naphthalocyanine is higher than that of phthalocyanine because of the increased π-electron conjugation due to additional benzoannulation.

1.9   TECHNOLOGICAL APPLICATIONS OF PHTHALOCYANINES AND NAPHTHALOCYANINES

Ever since the discovery of phthalocyanines, a rich and varied chemistry and technology has developed around these interesting material. This can be very well understood from thousands of patents and publications centered on phthalocyanines, and of late, on naphthalocyanines. In the early years of their discovery, they were mainly used as colourants in textiles, paints, printing inks and plastic materials. The non colourant applications include catalysis, analytical reagents, clinical diagnostic agents etc. After 1960's they have attracted wide attention because of their electrical, electronic, electrochemical, photovoltaic and thermo-optical applications. Of recent interest, in the burgeoning world of computers and information storage these materials are used as optical data recording media.[43]

The phthalocyanines assume importance in electrocatalysis[44] because they are structural and electronic analogues of porphyrins

whose electrochemistry is important in understanding electron transfer processes in biological systems. The photoconductivities and dark conductivities of phthalocyanines have been under investigation for several years, as a result of the interest in these materials for applications in photovoltaics, electrophotography, diodes, laser printers, photoelectrochemical devices, chemical sensors, and microelectronic devices.[45-49]

Cobalt(II) tetrasulphophthalocyanine (CoTSP) can be covalently bound to the surface of titanium dioxide particles. A reversible photochemical reduction of Co(II)TSP to Co(I)TSP is obtained when irradiated with light having energy exceeding the band gap energy of TiO_2 in presence of dioxygen. The photochemical stability and higher quantum yields of O_2 reduction makes these newly developed material applicable as a potent and stable oxidation catalyst. The advantages of this process is the simultaneous formation of dihydrogen and dioxygen from water. An overall transfer of conduction band electrons e^-CB and valence band holes h^+VB is necessary for the direct storage of solar energy in the form of chemical energy.

$$2H_2O \ + \ 2e^-CB \ \longrightarrow \ H_2(g) \ + \ 2OH^-(aq) \ \text{cathodic}$$

$$2H_2O \ + \ 4h^+VB \ \longrightarrow \ O_2(g) \ + \ 4H^+(aq) \ \text{anodic}$$

17
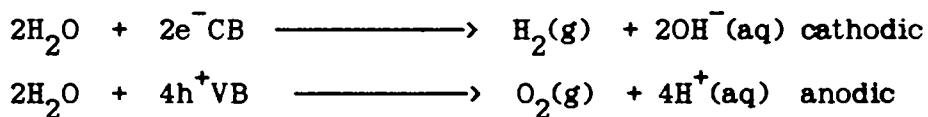
Cobalt tetrasulfophthalocyanine acts as an efficient electron relay to compete with the e^-/h^+ recombination and thus achieve reasonable quantum yields.

Electrochromic effect is the production of a colour change in materials localised at an electrode surface by faradaic reaction. Diphthalocyanine complexes of rare earth elements are of interest in view of their electrochromic properties.[50-54] A lutetium diphthalocyanine film exhibits four colour transitions: violet, blue, green and yellowish red when it is exposed to an electrolyte and the applied voltage is varied between ±1.5 V.[55-57]

In electrophotography electrically conductive substances are coated with photoconductive layers made up of phthalocyanine deposited in a binder resin.[58,59] Electrophotographic receptors may comprise of a photosensitive layer containing titanyl naphthalocyanine. These photoreceptors show good sensitivity towards long wavelength light from semiconductor lasers.[60]

Photodynamic therapy is a promising tool for the treatment of neoplastic diseases. 2,3-Naphthalocyanine satisfies several criteria for a photosensitizing agent. A photosensitizing agent should be in the spectral region where absorption by haemoglobin and other tissue absorbers and scattering by melanine and other

tissue scatterers are minimal. In addition it should be well matched by the output spectrum of a readily available laser beam and should be intense. The photosensitizing agent should have the necessary photophysical characteristics such as chemical stability and nontoxicity in the absence of light. It should also localise preferentially in target tissues and clear promptly from all tissues after it has served its function. 2,3-Metal naphthalocyanine complexes absorb light in the near-ir spectral region (750-850 nm) where tissue penetration is optimal and they have been suggested as strong candidates as photosensitizers in photodynamic therapy.[61-69]

Sulfonated derivatives of chloroaluminium and zinc 2,3 naphthalocyanines with various degrees of sulfonation were prepared by Firey *et al* [62] and their cellullar uptake, aggregation in cellular environments, cytotoxicity and photosensitizing properties were studied. Most of these are taken up by cells to satisfactory degrees and are not cytotoxic at the concentrations used. Among the samples studied only the least sulfonated samples of Zinc naphthalocyanine produced some phototoxic effect. Firey *et al* [63] have also found that silicon naphthalocyanine derivatives are relevant materials to the search for the second generation photodynamic therapy of cancer.

REFERENCES

1. Karaga, K; Tstsui, M. *Coord. Chem. Rev.* 1980, 32, 67.

2. Linstead, R.P. *J. Chem. Soc.* 1934, 1016.

3. Barrett, P.A.; Dent. C.E.; Linstead, R.P. *J. Chem. Soc.* 1936, 1719.

4. Leznoff, C.C.; Lever, A.B.P. *Phthalocyanines: Prospects and applications* ; VCH Publishers: New York, 1989.

5. Gulbinas, V; Chachisvilis, M; Persson, A.; Svasberg, S; Sundstrom, V. *J. Phys. Chem.* 1994, 98, 8118.

6. Kivits, P.J.; de Bont, M.R.J.; van der Veen, *J. Appl. Phys. A* 1981, 36, 101.

7. Burgess, A.N. *J. Appl. Phys.* 1987, 61, 74.

8. Bloom, A.; Burke, W.J. U. S. Patent, 4, 241, 355 (1980), Assignee:RCA.

9. Van der Veen, J.; Kivits, P.J.; de Bont, M.R.J. U. S. Patent 4, 298, 975(1981) Assignee: U. S. Philips Corp.

10. Japan Kokai Tokyo Koho, J 561 30742(1981) Assignee:Asahi Chemical Ind.

11. Hos, A.M.; Loutfy, R.O. *Thin Solid Films,* 1983, 106, 291.

12. Griffiths, C.H.; Iker, M.S. Goldstein, P. *Mol. Cryst. Liq. Liq. Cryst.* 1975, 33, 149.

13. Wheeler, B.L.; Nagasubramanian, G.; Bard, A.J.; Schechtman, L.A.; Dininny, D.R.;Kenny, M. E. *J. Am. Chem. Soc.* 1984, 106, 7404.

14. Wohrle, D.; Gitzel, J.; Krawezyk, G.; Tsuchida, E.; Ohno, H.; Okura, I.; Nishisaka, T. *J. Macromol. sci. Chem.* 1988, A25, 1227.

15. Sugano, T.; Ueno, N.; Watanabe, H. *Hyoumen* 1988, 26, 664.

16. Yanagi, H.; Ashida, M.; Elbe, J.; Wobrle, D. *J. Phys. Chem.* 1990, 94, 7056.

17. *"Molecular Semiconductors"*, Simon, J.; Andre, J.J. (Eds.) Springer–Verlag, New York, 1985.

18. Wobrle, D.; Meissner, D. *Adv. Mater.* 1991, 3, 129.

19. Kapalan, M.L.; Louinger, J.A.; Reents, W.D.; Schmidt, P.H. *Mol. Cryst. Liq. Cryst.* 1984, 12, 345.

20. Thomas, A.L.; Moser, F.H. (Ed) *The Phthalocyanines*, 1983, Vol I.

21. Shramm, C.J.; Scaringe, R.P.; Stojakovic, D.R.; Hoffmann, B.M.; Ibers, J.A.; Marks, T.J. *J. Am. Chem. Soc.* 1980, 102, 6702.

22. Dent, C.; Linstead, R.;Lowe, A. *J. Chem. Soc.* 1934, 1033.

23. Byrne, G.; Linstead, R.; Lowe, A. *J. Chem. Soc.* 1934, 1017.

24. Linstead, R.; Lowe,A. *J. Chem. Soc.* 1934, 1022.

25. Barret, P.A.; Dent, C.E.; Linstead, R.P. *J. Chem. Soc.* 1936, 1719.

26. Kirin, I.S.; Moskalev, P.N.; Makashev, Y.A. *Russ. J. Inorg. Chem.* 1967, 12, 369.

27. Walton, D,; Ely,B.; Elliot,G. *J. Electrochem. Soc.* 1981, 128 (11), 2479.

28. M'Sadak, M.; Roncali, J.; Garnier, F. *J. Eletroanal. Chem.* 1985, 189, 99.

29. Luk'yanets, E.A.; Puchnova, V.A.; Mikhalenko, S.A.; Ruzina, S. G. U. S. S. R. No. 232, 963; Byull Izobset., No. 2, 28, 1969.

30. Bradbrook, E.F.; Linstead, R.P. *J. Chem. Soc.* 1936, 1744.

31. Luk'yanets, E.A.; Mikhalenko, S.A; *Zh. Obshch. Khim.* 1969, 39 (11), 2554.

32 Dent, C.E.; Linstead, R.P. *J. Chem. Soc.* 1934, 1027.

33. Walton, D.; Ely, B.; Elliott, G. *J. Electrochem. Soc. Solid-state Sciences and Technology,* 1981, 128, 2479.

34. Robertson, J.M.; Linstead, R.P.; Dent, C.E. *Nature,* 1935, 135, 506.

35. Robertson, J.M. *J. Chem. Soc.* 1935, 615.

36. Robertson, J.M.; Woodword, I.J. *J. Chem. Soc.* 1937, 219.

37. Easter, J.W. (To American Cyanamid Co.) U.S. Patent 2, 770, 629 (1956).

38. Anderson, J.S.; Bradbrook, E.F.; Cook, A.H.; Linstead, R.P. *J. Chem. Soc.* 1938, 1151.

39. Lucia, E.A.; Verderame, F.D. *J. Chem. Phys.* 1968, 48, 2674.

40. Mikhalenko, S.A.; Lukyanets, E.A.; *Wn. Obschi. Khim.* 1969, 39, 2554.

41. Paterson, J.L.; Schram, C.S.; Stojakovik, D.R.; Hoffman, B.M.; Marks, T.J. *J. Am. Chem. Soc.* 1977, 99, 286.

42. Marks, T.J.; Kalina, D.W.; Miller, J. (Ed) *Extended linear chain Compounds,* 1982, 197.

43. Kivits, P.; de Bont, R.; van der Veen *J. Appl. Phys.* 1981, A26, 101.

44. Simon, J; Tournilhae, F. *New. J. Chem.* 1987, 11, 383.

45. Worhle, D; Meissner, D. *Adv. Mater.* 1991, 3, 129.

46. Klofta, T.; Sims, T.D.; Pamkow, J.W.; Danziger, J.; Nebersny, K.W.; Armstrong, N.R. *J. Phys. Chem.* 1987, 91,   5651.

47. Brina, R.; Collins, G.F.; Lee, P.A.; Armstrong, M.R. *Anal. Chem.* 1990, 62, 2367.

48. Danziger, J.; Dodelat, J.P.; Armstrong, N.R. *Chem. Mater.* 1991, 3, 812.

49. Williams, W.S.; Sokoloff, J.P.; Ho, Z. Z.; Arbour, C.; Peyghambarian, N. *Chem. Phys. Lett.* 1992, 193, 317.

50. Moskalev, P.N.; Kirin, I.S. *Russ. J. Phys. Chem.* 1972, 46, 1019.

51. Kirin, I.S.; Moskalev, P.N.; Makashev, Yu. A.; *Russ. J. Phys. Chem.* 1965, 10, 1065.

52. Kirin, I.S.; Moskalev, P.N.; Makashev, Yu. A.; ibid., 1967, 12, 369.

53. Misumi, S.; Kasuga, K.; Nippon Kagaku Zasshi, 1971, 92, 385.
    54. Mac Kay, A.G.; Boas, J.F.; Troup, G.J. *Aust. J. Chem.* 1974, 27, 955.

54. Nicholson, M.M.;Galiardi, R.V. Final Report, Contract 62269, May 1977.

55. Moskalev, P.N.; Kirin, I.S. *Opt. Spectrosc.* 1970, 29, 220.

56. Nicholson, M.M.; Pizzasello, F.A. *J. Electrochem. Soc.* 1980, 821.

57. La Mar. G.N.; Jeffery, S.R.; Smith, K.M.; Langry, K.C. *J. Am. Chem. Soc.* 1980, 102, 4835.

58. Royo Ink Mfg. Ltd. Jpn. Kokai Tokyo, Koho JP 59, 116, 754, 1982. CA 1985, 123055d.

59. Fuji Xerox Co. Ltd. Jpn. Kokai Tokyo, Koho JP 0162, 667, 1989, CA 1990, 66649f.

60. Mitsubishi Petrochemical Co. Ltd., Jpn. Kokai Tokyo, Koho JP 02, 79, 046, 1990, CA 1990, 162512x.

61. Kriemer-Bisnbaum, M. *Semin. Hematol.* 1989, 26, 157.

62. Firey, P.A.; Rodgers, M.A.; *J. Photochem. Photobiol.* 1987, 45, 535.

63. Firey, P.A.; Jones, T.W.; Chang, H.Y.; Kenney, M.E.; Rodgers, M.A. J. NATO ASI Ser., Ser. H 1988, 15, 77.

64. Firey, P.A.; Forel, W.E.; Sounik, J.R.; Kenney, M.E.; Rodgers, M.A. *J. Am. Chem. Soc.* 1988, 110, 7626.

65. Yates, N.C. NATO ASI Ser., Ser. H1988, 15, 365.

66. Ford, W.E.; Rihter, B.D.; Kenney, M.E.; Rodgers, M.A. *J. Am. Chem. Soc.* 1989, 11, 2362.

67. Cumo, V.; Jori, G.; Kenney, M.E.; Rodgers, M.A. J. *Br. J. Cancer* 1990, 62, 966.

68. Henderson, B.W.; Mayhew, E. *Proc. SPIE-Int. Soc. Opt. Eng.* 1990, 1203, 126.

69. Paquette, B.; Owllet, R.; Ali, H.; Langloir, R.; van Lier, J. E. *Proc. SPIE Int. Soc. Opt. Eng.* 1990, 1203, 246.

CHAPTER II

EXPERIMENTAL

Abstract

This chapter discusses the experimental techniques employed in these studies. The procedures for the synthesis of metal free naphthalocyanine [H_2Nc] vanadyl naphthalocyanine [VONc], zinc naphthalocyanine [ZnNc], europium dinaphthalocyanine [$Eu(Pc)_2$], and europium diphthalocyanine [$Eu(Pc)_2$] and their purification are also presented. The compounds were characterized by elemental analysis and uv-vis and ir spectra. Since the compounds have already been reported, only the qualitative characterization is presented.

2.1 INTRODUCTION

Only very few test tube reactions were carried out by Linstead and co-workers[1] during the early days of the discovery of 2,3-naphthalocyanine probably due to the scarcity of the starting material 2,3-dicyanonaphthalene. Most of their studies were concentrated on 1,2-naphthalocyanines, a more accessible material. 1,2-Naphthalocyanine so obtained was a mixture of several isomers that were difficult to separate. However, in recent years most of the work is concentrated on 2,3-naphthalocyanine because of its better properties for applications. 2,3-Naphthalocyanine synthesized contains only a single isomer.[2] Generally 2,3-naphthalocyanines are synthesized by heating 2,3-dicyanonaphthalene with the appropriate metal or metal compound. The reaction is carried out in a sealed, evacuated tube after flushing with nitrogen.

Purification of the product has been accomplished by exhaustive soxhlet extraction with suitable solvents followed by vacuum sublimation. 2,3-Naphthalocyanines are not amenable to recrystallization from common solvents and in the present study they were used after purification by liquid chromatography

27

2.2 SYNTHESIS AND PURIFICATION

2.2.1 Metal free naphthalocyanine (H_2Nc)

Metal free naphthalocyanine was prepared from magnesium naphthalocyanine which, in turn, was prepared from magnesium powder and 2,3-dicyanonaphthalene(2,3-DCN). In a typical preparation 0.2 g of magnesium powder and 2.0 g of DCN were ground together to form an intimate mixture. The mixture was sealed in a nitrogen flushed thick walled glass ampoule and heated at 370^0C for 80 minutes. The crude magnesium naphthalocyanine so obtained was washed with acetone and ethanol and then dissolved in con.H_2SO_4 and poured over ice to precipitate metal free naphthalocyanine.

H_2Nc so obtained was purified by exhaustively extracted with acetone in a micro soxhlet extractor and dried at 100^0C in vacuum.

2.2.2 Vanadyl naphthalocyanine (VONc)

A mixture of 0.1 g of V_2O_5 and 0.2 g of 2,3-DCN was heated to 300^0C in an evacuated glass ampoule for 45 min. VONc so formed was stirred with dil.HCl for 24h to dissolve unreacted V_2O_5. Then it was soxhlet extracted with acetone and dried at 120^0C in vacuum.

28

2.2.3 Zinc naphthalocyanine (ZnNc)

Anhydrous zinc acetate and 2,3-DCN were mixed in the weight ratio 1:4 in an evacuated glass tube after flushing with nitrogen. The mixture was heated to $250^{0}C$ for 2 h in a furnace. ZnNc formed was powdered and stirred with dil.HCl to dissolve unreacted zinc acetate. Then it was soxhlet extracted with ethanol and acetone and dried in vacuum at $100^{0}C$ for 2 h.

2.2.4 Europium dinaphthalocyanine [Eu(Nc)$_2$]

A mixture of 0.14 g of anhydrous europium acetate and 0.68 g of 2,3-DCN were heated to $250^{0}C$ for 2h in a nitrogen flushed evacuated glass tube. Eu(Nc)$_2$ thus synthesized was dissolved in DMF and column chromatographed over neutral alumina using DMF as eluent. DMF was evaporated off and Eu(Nc)$_2$ was dried at $130^{0}C$ in *vacuo* for 4 h.

2.2.5 Europium diphthalocyanine [Eu(Pc)$_2$]

Anhydrous europium acetate and phthalonitrile were mixed in the stoichiometric ratio 1:8 and heated to $280^{0}C$ in a nitrogen atmosphere for 2 h. The product was column chromatographed over neutral alumina using DMF as eluent.

2.3 DOPING OF SAMPLES WITH IODINE

The naphthalocyanines and phthalocyanines were doped with iodine in the solution phase. Resublimed iodine was used for the doping of samples. Finely powdered sample (0.2g) was stirred with a 50 ml. of saturated solution of iodine in dry carbon tetrachloride for 24 h. Then it was filtered and washed several times with carbon tetrachloride till the filtrate was completely free from iodine. The doped samples were dried in a desicator and stored in stoppered glass bottles.

Iodine from the doped sample was extracted by the oxygen flask method using platinum as catalyst. The oxidation product was collected by shaking with 20 ml. of 2 M potassium hydroxide. The sample was transferred to standard flask. Aliquots were withdrawn and acidifeid using sulfuric acid. The iodide was determined by its ability to catalyze the reduction of ceric ions by arsenious acid. The rate of reaction is proportional to the amount of iodide present. The reaction was stopped at specific time intervals by the addition of ferrous ammonium sulfate. The ferric ion concentration was measured spectrophotometrically using potassium thiocyanate as reagent.

2.4 CHARACTERIZATION

2.4.1 Absorption Spectra

The uv-vis absorption spectrum of metal free naphthalocyanine was recorded in 90% sulfuric acid. For the other materials the spectra was recorded in DMF solutions using a Shimadzu uv-vis spectrophotometer UV-160A.

The uv-vis spectral characteristics of different samples are given in Table 2.1.

Table 2.1   UV-VIS spectral characteristics of different naphthalocyanines and europium diphthalocyanine

Sample	Observed λ_{max}(nm)	Reported λ_{max}(nm)	Reference
H_2Nc	762	756	2
VONc	797	820	2
ZnNc	784	780	3
$Eu(Nc)_2$	763	766	4
$Eu(Pc)_2$	626	629	5

The slight variations in the observed λ_{max} probably arise out of the effect of solvent.

2.4.2 Infrared Spectra

The ir spectrum of the samples were recorded using FTIR Spectrophotometer (DR-8001, Shimadzu) in KBr pellets. The main ir absorption peaks are given in Table 2.2.

Table 2.2 IR absorption peaks of naphthalocyanines and europium diphthalocyanine

Samples	Infrared Spectra λ_{max} cm^{-1}
ZnNc	1335, 1095m, 1026, 752
VONc	1370, 1088, 1026, 756
H$_2$Nc	1385, 1091, 1028, 887, 754
Eu(Nc)$_2$	1387, 1089, 1024, 889, 754
Eu(Pc)$_2$	1385, 1016, 432

In naphthalocyanines, a strong line at 1085-1095 cm^{-1} can be assigned to the in-plane naphthalocyanine ring vibration due to conjugated C-C and C-N stretching. The peak at 1385 cm^{-1} is also due to C-C and C-N stretching vibrations in the macrocyclic ring. The band at 1024-1028 cm^{-1} may be due to the in plane C-H vibrations. The peak at 887-889 cm^{-1} are assigned to out-of-plane C-H bending vibrations in naphthalene rings. The peak at 752-754 cm^{-1} is also due to out-of-plane C-H bending vibrations.

In the case of europium dinaphthalocyanine, the peak at 1385 cm^{-1} is due to the C-C and C-N stretching vibrations. The in plane C-H vibrations of the macrocyclic ring may be the cause of 1016 cm^{-1} band.

The ir spectra are in good agreement with those reported earlier.

2.5   EFFECT OF DOPING

The doping procedure was carried out as described in section 2.3. This procedure avoids any possibility of retaining adsorbed iodine on the material. The preheating in vacuum further confirms the absence of any loosely bound iodine on the solid surface. The stoichiometry of the doped forms is presented in Table 3.1

Table 3.1 Stoichiometry of doped samples

Compound	Stoichiometry of doped form
H_2Nc	$H_2Nc\ I_{0.11}$
VONc	$VONc\ I_{0.12}$
ZnNc	$ZnNc\ I_{0.12}$
$Eu(Nc)_2$	$Eu(Nc)\ I_{0.02}$
$Eu(Pc)_2$	$Eu(Pc)_2 I_{0.02}$

REFERENCES

1. Bradbrook,E. F.; Linsted, R.P. *J.Chem.Soc.* 1936, 1744.

2. Kaplan, M. L.; Lovinger, A. J.; Reents, W. D. JR.; Schmidt, P.H. *Mol. Cryst. Liq. Cryst.* 1984, 112, 345.

3. Yanagi, H.; Kouzeki, T.; Ashida, M.; Noguchi, T.; Manivannan, A.; Hashimoto, K.; Fujishima, A. *J. Appl. Phys.* 1992, 71,(10), 5146.

4. Mikalenko, S.A.; Lukyanets, E.A. *Zh. Obsch. Khim.* 1969, 39, 2554.

5. Kirin, I. S.; Moskalev,P.V.; Makashev, Yu. A. *Russ. J. Inorg. Chem.* 1967, 12(3), 369.

3.1   INTRODUCTION

The prerequisites for organic semiconductors to exhibit electrical conductivity are an ordered conjugated structure with extended π-electrons and a large carrier concentration. The fundamental processes of charge carrier formation and migration in model macrocyclic metal complexes like metal phthalocyanines and naphthalocyanines are important to understand the mechanism of electron transfer in biological systems. Extensive research into the semiconductor properties of metal porphyrins, phthalocyanines, chlorophyll and their analogues has been conducted by Vartanyan.[1-4]

The electrical conductivity of phthalocyanines and naphthalocyanines can be improved by doping them with dopants like iodine.[5] In the chemical sense, they can be considered as salts formed by their organic precursors and small molecules of inorganic oxidants. They are said to be "organic metals" which represent a group of charge-transfer complexes. When a charge-transfer complex is formed, electrons are transferred from the donor organic precursor to the acceptor compound. In the crystal of an "organic metal" the flat organic molecules are partially oxidized and form stacked arrays whereas small inorganic anions occupy the cavities between the bulky molecular array.

In the quasi—one-dimensional picture, each donor molecule supplies its highest occupied molecular orbital (HOMO) to form a one-dimensional band and the parameters of one electron hopping between the HOMOs of the two adjacent molecules in the stack is directly related to the bandwidth. In the process of crystal formation some part of electrons moves to the acceptor molecule and each donor unit acquires an average positive charge. In the case of iodine doped phthalocyanines (MPcI), the iodine atoms form the linear I_3^- anions in the channel between the MPc stacks. Each I_3^- unit captures one electron fron the donor stack and the average charge of a molecule is 1/3.[6] The stoichiometry of the charge transfer complex, in fact, depends on the method of its preparation. However iodine-doped phthalocyanine H_2PcI illustrates conclusively that a central metal ion is not required for high electrical conductivity.[7]

Bufler et al [8] have described the electronic structure of rare earth based phthalocyanine dimers with $LuPc_2$ as a typical example. In these narrow-band semiconductors the two Pc rings are separated by 0.3 nm with a central metal ion (M^{3+}). The charge of the central metal ion is compensated by one or two electrons from the macrocyclic ring. The π-electrons of the aromatic system mainly govern the electronic properties of the material. The macrocyclic ligand consists of four isoindole groups joined by aza groups. The

orbitals of the central metal atom do not contribute to the electrical properties of the system because they are energetically well below the highest occupied molecular orbital (HOMO) of the aromatic system.[9] The molecule can be individually oxidised and reduced due to the radical nature of $LuPc_2$. The anions and cations formed during the charge transfer reaction are responsible for the electrical conductivity.

The temperature dependence of electrical conductivity can be expressed by the Arrhenius relationship,

$$\sigma = \sigma_o \exp(-Ea/2kT)$$

where

σ – specific conductivity at temperature T expressed in S cm^{-1}

σ_o – specific conductivity at infinite temperature

Ea – activation energy for conduction

k – Boltzmann constant.

The activation energy Ea, the most important characteristic of an organic semiconductor determines the minimum energy required to produce a charge carrier in the solid matrix.[10,11] The methods of sample preparation and purification affect Ea. This can be well understood from the fact that the value for Ea for H_2Pc reported by

different investigators using samples prepared by different methods. The value varies from 1.7 eV for single crystals and vacuum deposited thin layer to 0.9 eV for a thick layer deposited by smearing on a quartz substrate.[12] The difference in the value of Ea is due to the different intermolecular and crystalline interactions. Hence it is necessary to prepare samples under identical condition for the evaluation of conduction parameters.

Scanning through the literature it is seen that the electrical properties of 2,3-naphthalocyanines have received only scant attention. Some very sketchy data has been published for 1,2-naphthalocyanines.[13] The activation energy for conductivity in 1,2-CuNc is reported as 0.72 eV. Also Wachawek *et al*[14] reported the sensitivity of conductivity of 1,2-Ncs to the surrounding atmosphere. A study of the conductivity of amorphous 1,2-CuNc grown directly on brass substrate was published by Gudkov *et al.*[15]

Shimura *et al* [16] have reported the activation energy of carrier formation in MgNc thin films deposited on glass plates to be 0.30 eV. They have shown that carrier mobility of MgNc thin films after heat treatment increases substantially. Deger *et al*[17] have compared the room temperature dc conductivity of 2,3-FeNc and FePc and showed that 2,3-FeNc has electrical conductivity four orders of magnitude greater than that of FePc.

3.2 EXPERIMENTAL

3.2.1   Electrical conductivity measurements

The electrical conductivity measurements were carried out in an electromagnetically shielded cell described in Figure 3.1. Finely powdered samples were pressed at 3000 kg/cm^2 to form pellets of 5 mm diameter and about 2 mm thickness. These pellets were used for electrical conductivity measurement.

3.2.2   Fabrication of shielded cell for electrical conductivity measurements

A schematic diagram of the variable temperature cell used for the study of electrical properties of solid samples is shown in Figure 3.1. This cell was fabricated incorporating the desirable features of the cell reported in literature.[18-21] A unique feature of this design is that the cell can be used for programmed temperature from 80 K to 450 K without disrupting the vacuum. Also the cell can be used for measuring electrical conductivity and dielectric constant. Provisions were also incorporated for studying photoconductivity of the samples.

41
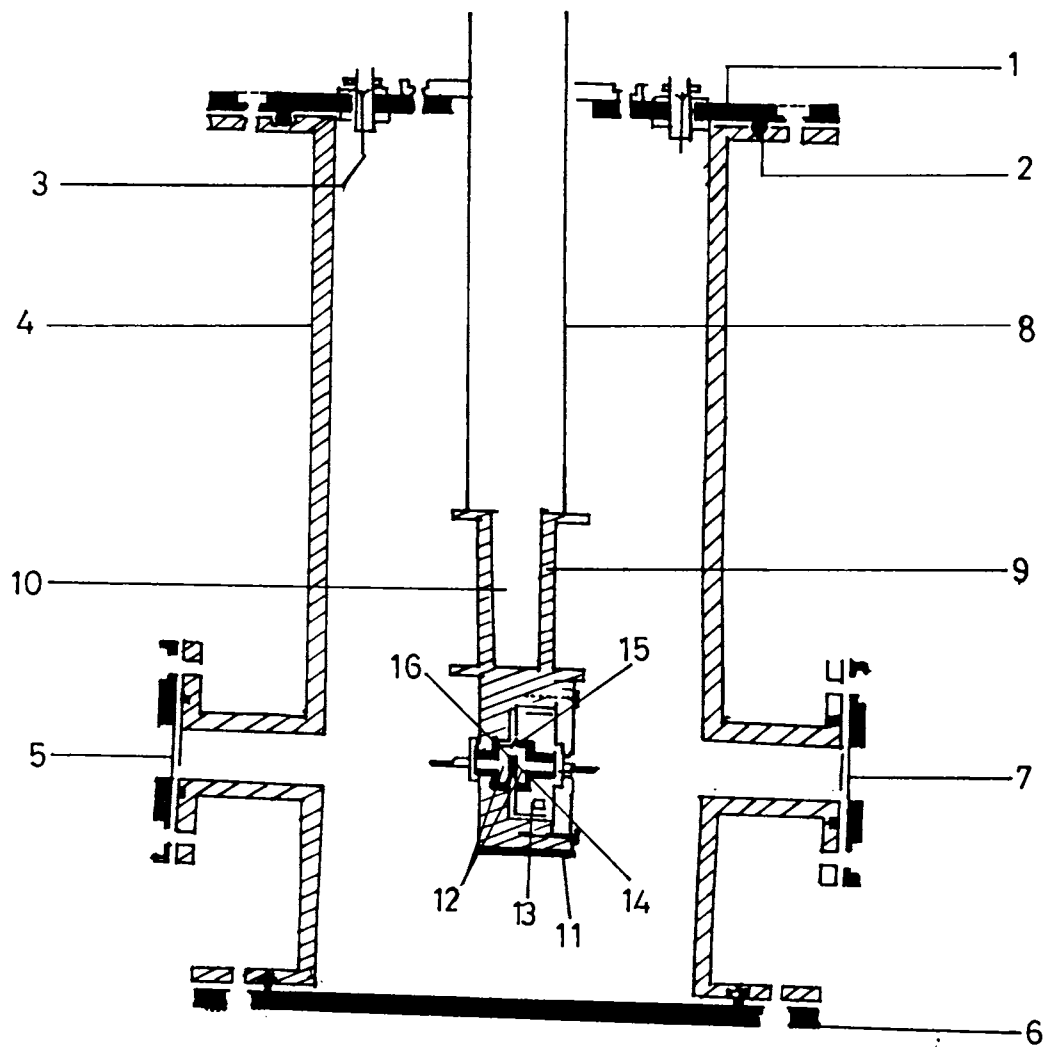
1.	Top plate	9.	Copper cold finger
2.	Neoprine O-ring	10.	Liquid nitrogen cavity
3.	BNC	11.	Heater coil
4.	MS body	12.	Electrodes
5.	View port	13.	Dismountable ram
6.	Base plate	14.	Teflon insulation
7.	To vacuum	15.	Thermocouple
8.	SS tube	16.	Sample

Fig.3.1   Schematic diagram of the variable temperature cell used for the measurement of electrical properties of solids.

The cell consists of an MS cylinder whose ends are permanently fixed with MS flanges. For vacuum sealing, these flanges are provided with O-ring grooves. This chamber is sealed by top and bottom covers using neoprene O-rings. The top cover is provided with six insulated leads. These leads are connected to the conductivity electrodes, thermocouple and dc power supply for heating element. Four window ports were provided to the chamber for the following uses: (i) for coupling with rotary pump for evacuating the chamber (ii) for carrying out photoconductive experiments (iii) to visually inspect the specimen for any change during heating.

The sample holder consists of a cylindrical copper block, one end of which is shaped as a rectangle. The cylindrical end is bored to a depth such that the rectangular block holding the electrodes is 4 mm below the end of the bore. A dc heating element is accommodated at the end of the rectangular block. At the centre of the rectangular block is a teflon-insulated circular gold coated copper electrode of 12 mm diameter. Another movable copper block of the same dimension fixed with teflon-insulated gold plated copper electrode of the same diameter serves as the second electrode. The second electrode is screwed on to the rectangular block such that the axes of the two circular electrodes are

perfectly aligned, and are kept under tension using springs. A thermocouple well is provided in the fixed block and the thermocouple is inserted through a ceramic insulator. The tip of the thermocouple is placed very close to the electrode so that the temperature of the sample can be monitored with a fair degree of fidelity. The top end of the copper cylinder is silver brazed to a SS tube of the same diameter. This SS tube is permanently fixed to an MS flange. This cold finger assembly is inserted through the top plate of the cell and is fixed on to this plate using an O-ring and tightened with allen screws. The length of the SS tube is adjusted such that the geometrical centre of the copper electrode is in a line with the axis of the windows. The electrical connections for thermocouples, heaters, and the electrodes are made through teflon-insulated connectors provided through the top plate.

The major advantages of the cell design are:

1. The cell can be used to measure electrical conductivity of the samples in the temperature range 80 K to 500 K without disrupting the vacuum within the cell.

2. The cell can be used to measure photoconductivity of samples just by changing the electrode configuration.

3. The liquid nitrogen needed for measurement is small for a single cycle operation.

4. The cell can be used for measurement up to 10^{-4} Torr.

5. DC heating facility minimizes noise from the heating coils, and the outer metal cylinder which is earthed acts as a shield for electromagnetic waves.

3.2.3   Electrical circuit

The sample was mounted between the electrodes in the cell. For the resistance measurement mode, the two terminals were connected to an electrometer (Kiethly Model 617). The built-in potential source of the electrometer was connected in series in the circuit. Using this electrometer, current as low as 10^{-15}A could be measured. The terminals of the thermocouple were connected to a digital multimeter with readability of 10 μV. Heating of the sample was controlled by a dc power supply. The heating programme was calibrated using dummy samples and the programme was controlled manually.

The ac conductivity measurements were carried out using an

45

impedence analyser (Hewlett-Packard 4192 A LF Impedence analyser). The sample was mounted in the cell and the sample leads were connected to the impedence analyser assuming that the resistance of the leads are negligible. An exciting input of suitable frequency and amplitude was applied between the electrodes and the impedence was directly measured. The ac conductivity was evaluated from the relationship

$$\sigma_{ac} = \frac{1}{I} \times \frac{d}{A}$$

where I is the impedence, d is the thickness of the sample and A is the area of the sample in contact with the electrode.

All measurements were made with the sample in a dynamic vacuum unless otherwise specified. The measurements were repeated several times to ensure reproducibility.

3.3   DC CONDUCTIVITY STUDIES

Among the electrical properties of materials the parameter which can be easily evaluated is the dc conductivity. Using an electrometer and a shielded cell the dc conductivity can be measured in a wide range. The phase transitions of samples can also be identified from the temperature dependent dc conductivity

studies.

The rate of flow of carriers across the sample in applied dc field is represented by the dc conductivity. The flow of carriers across the sample, in turn, depends on the mobility of carriers and the density of states associated with conduction. The temperature dependance of dc conductivity is given by the Arrhenius equation,

$$\sigma_{dc}(T) = \sigma_o \exp(-Ea/2kT)$$

From the above equation it can be seen that plot of dc conductivity versus inverse of temperature is linear and with a slope equal to Ea/2k. A linear dependence is obtained in the case of samples in the crystalline phase whereas the dependence of σ_{dc} on temperature assumes a different format for a disordered sample. Thus from the nature of dependence of dc conductivity on temperature, the mechanism of conduction of the sample can be delineated.

Kaplan *et al* [22] have measured the room temperature dc conductivity of H_2Nc, PbNc and VONc compressed pellets. All naphthalocyanines reported exhibit semiconducting behavior. A considerable decrease in the resistivity of H_2Nc compared to PbNc and VONc was observed in their experiments. The low resistivity of

H_2Nc was accounted by the method by which H_2Nc was synthesized. They have observed that when an additional dopant is added to H_2Nc, the resistivity does not decrease but increased by a factor of 10. They doped the samples using bromine vapour. The resistivities of PbNc and VONc decreased on doping with bromine by about an order of magnitude.

Pressed pellets of H_2Nc, VONc, ZnNc, $Eu(Nc)_2$, and $Eu(Pc)_2$ both pristine and iodine doped samples were selected for dc conductivity studies. Logarithm of dc and ac conductivity as a function of temperature of the above samples are shown in Figures 3.2 to 3.17. Every sample studied was heated to 370 K and cooled to ambient temperature before the start of measurement to avoid the interference of moisture and adsorbed oxygen. It is seen that in most cases, iodine doping of phthalocyanines and naphthalocyanines increases the conductivity. The presence of any adsorbed iodine in doped samples is ruled out since the conductivities were measured after annealing the sample to 370 K in vacuum.

A number of reports have been published regarding the mechanism of conduction in phthalocyanine samples doped with iodine.[23-25] Iodine is an advantageous oxidant for planar organic molecules because of the high stability of I_3^- in nonpolar environments and because of the ability of I_3^- to accommodate

itself to channels in one-dimensional lattices.[26,27] According to Equation 3.1, a divalent metal complex would produce a trivalent metal ion if I^- were produced, but a nonintegral oxidation state if all sites in the material were crystallographically similar and if only I_3^- were formed, eg. $(LM)(I_3^-)_{1/3}$ where M has a formal oxidation state of 2.33.

$$(L)M \quad + \: 1/2 \: nI_2 \quad \longrightarrow \quad (LM)(I)_n \quad \text{——— (3.1)}$$
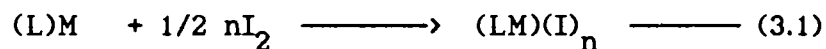
It is possible to create nonintegral oxidation state in naphthalocyanine and phthalocyanine using iodine as oxidant. The dopant iodine forms a charge-transfer complex with these compounds. Most of the reports suggest stacks of MPc^{+x} cations and parallel chains of disordered I_3^- counter ions.

$$MPc \quad + \quad 1/2 \: nI_2 \quad \longrightarrow \quad MPc(I)_n$$
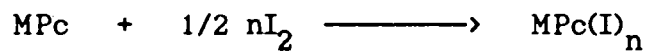
3.4 AC CONDUCTIVITY

In dc conductivity studies, only the net charge which traverses the entire sample is measured, whereas in ac conductivity measurements, the electrical conductivity is measured as a function of an alternating field. The changes in the character of the material affecting its polarizability are also reflected in ac

conductivity results.

3.5 RESULTS AND DISCUSSION

In accordance with the observation of Kaplan *et al*,[22] the conductivity of H_2Nc is significantly higher than that of metal naphthalocyanines. This difference in conductivity of H_2Nc may be due to the method by which it was prepared.[22] The H_2Nc sample was prepared from MgNc which, in turn, was synthesized from 2,3-dicyanonaphthalene. MgNc was dissolved in concentrated sulfuric acid and poured over ice to precipitate H_2Nc. Some oxidation might have occurred during this step and such species contaminate the product acting as an impurity dopant and can modify the electrical conductivity.

The temperature dependence of σ_{dc} from 100 K to 450 K for the metal free and iodine doped metal free naphthalocyanine are depicted in Figure 3.2. Both the samples show only a very weak temperature dependence upto about 200 K. Such weak temperature dependence of σ_{dc} is characteristic of a mechanism involving hopping of charge carriers in a manifold of states at the Fermi level.[28,29] Above that temperature the samples obey Arrhenius relation. The activation energy evaluated are 0.14 eV and 0.1 eV for pristine and doped samples respectively.
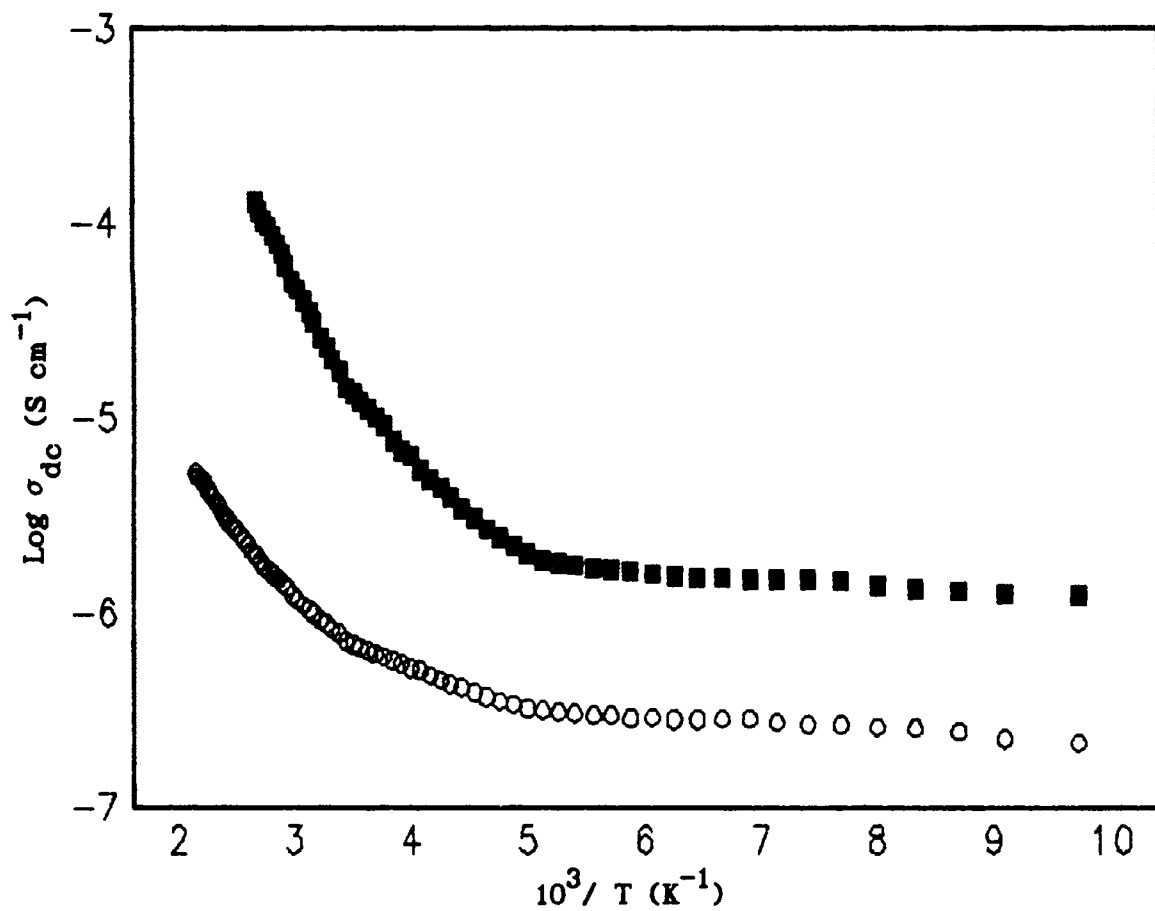
50

Fig.3.2   Log σ_{dc} versus $10^3/T$ plot of H_2Nc in the pristine and iodine doped compressed pellets.

O H_2Nc ■ H_2NcI

Kaplan *et al* have reported that the conductivity of bromine-doped samples decreases by an order of magnitude. This difference may be due to the difference in the extent of oxidation that takes place during doping of the sample. Also bromine may bring about a partial substitution on the aromatic ring. Such ring substituted H_2Nc is likely to show a lower conductivity.

The temperature dependence of σ_{ac} for H_2Nc and H_2NcI at selected frequencies are shown in Figures 3.3 and 3.4. Measurement of σ_{ac} could not be made at lower frequencies probably due to high dc conductivity.[30] The σ_{ac} measurements were carried out only above 300 K since noticeable dependence was observed only at that temperature. The temperature as well as frequency dependence of σ_{ac} does not help to distinguish the conventional mechanisms that have been put forward for explaining the conduction in quasi-one-dimensional systems like polyacetylene. Probably a combination of hopping mechanism prevails.

Iodine-doped samples show higher conductivity than the pristine samples. The mobility of the charge carriers becomes activated when the temperature exceeds the phonon temperature characteristic of the highest energy phonons with which the electronic states interact appreciably.
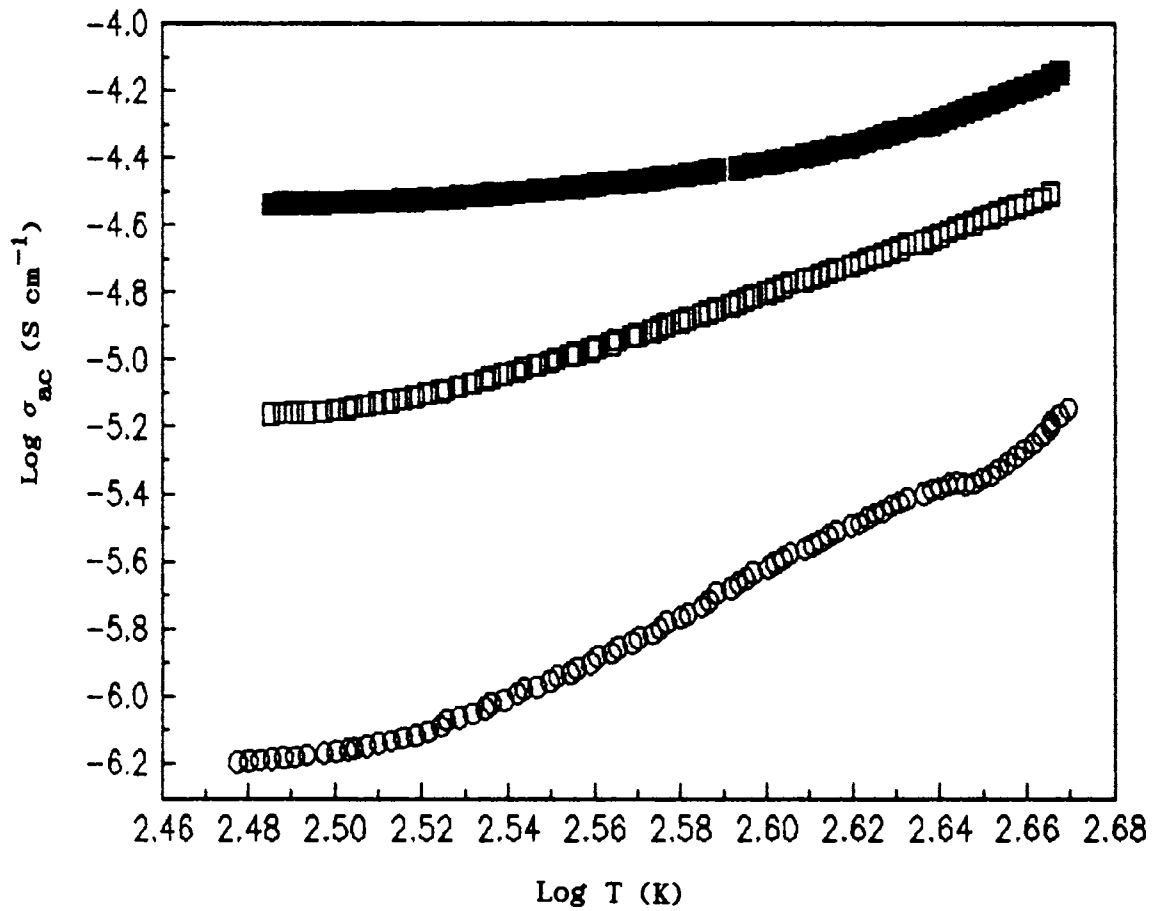
52

Fig.3.3   Plot of log σ_{ac} versus log T at three different frequencies of H_2Nc pellet.

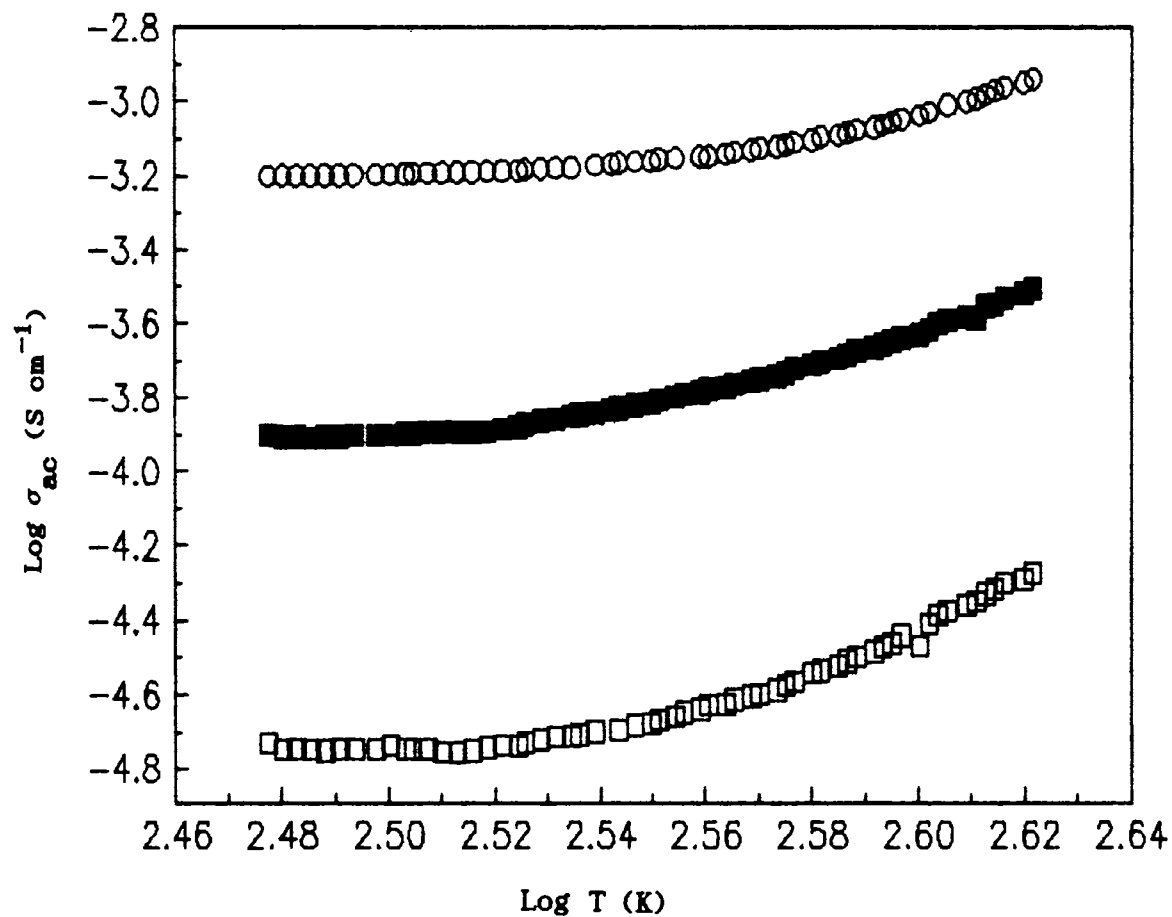■   1 MHz   ☐   100 KHz

O   1 KHz

53

Fig.3.4   Plot of log σ_{ac} versus log T at three different frequencies of H_2NcI.

O   5 MHz   ■   1 MHz

◻   100 KHz

The Arrhenius plot for the temperature dependence of σ_{dc} for VONc and iodine-doped VONc are represented in Figure 3.5. In the pristine sample temperature dependence is very weak below about 300 K. Above that temperature the behaviour is in accordance with Arrhenius equation and the transition around this temperature points to a change in mechanism of conduction. The increase in conductivity at higher temperature may be due to the increase in carrier density with increase in thermal energy. The behaviour of iodine-doped VONc indicates that considerable change has occurred in the electronic environment of the molecule as a result of doping. This is confirmed by the change in activation energy from 0.1 eV to 0.05 eV.

The temperature dependence of σ_{ac} for pristine and iodine-doped VONc are given in Figures 3.6 and 3.7. In VONc log σ_{ac} versus log T, approaches a straight line especially at higher temperature indicating a thermally activated hopping in the band tails. Its frequency dependence is also empirically in conformity with the mechanism which may be be given by the expression[31]

$$\sigma_{ac} = f^{S} \, T \, \exp \, (-Ea/kT)$$

55
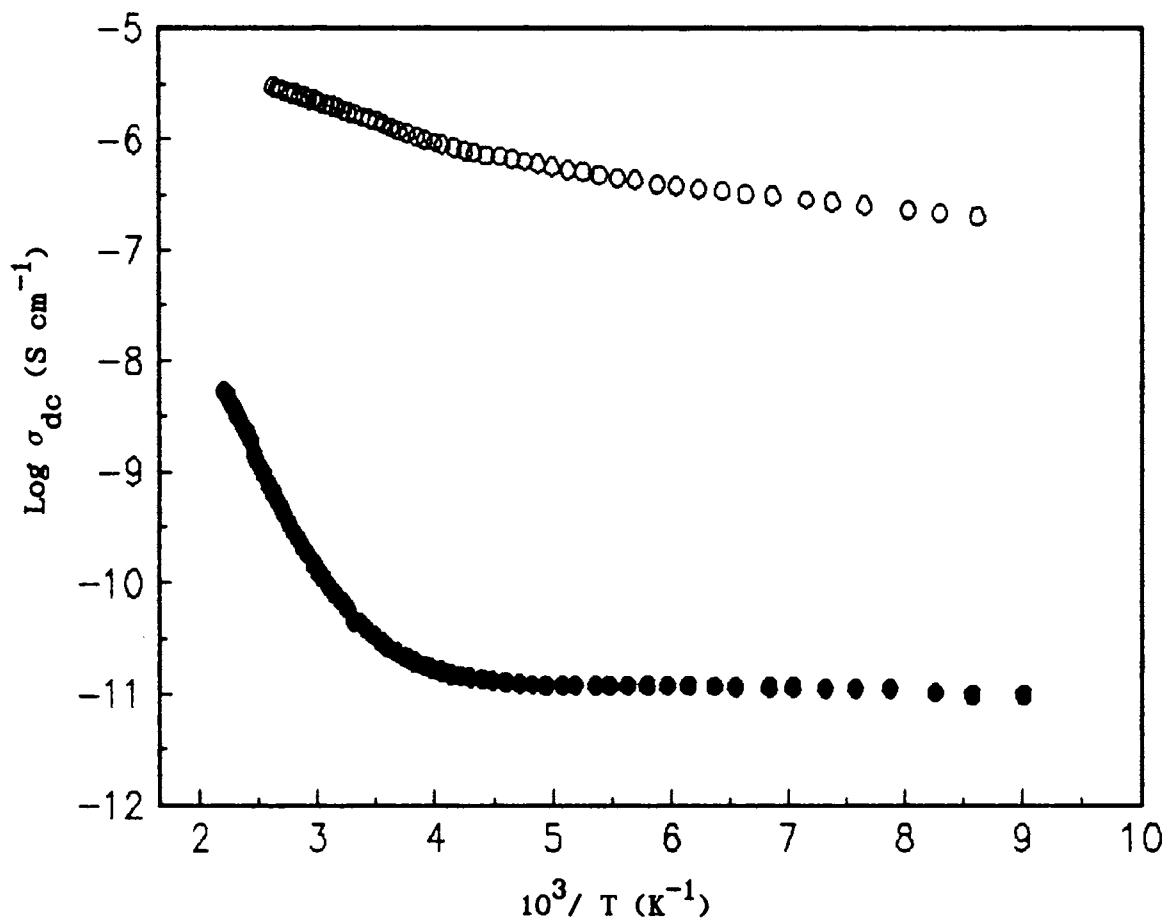
Fig.3.5   Log σ_{dc} versus $10^3/T$ plot of pristine and iodine doped
VONc

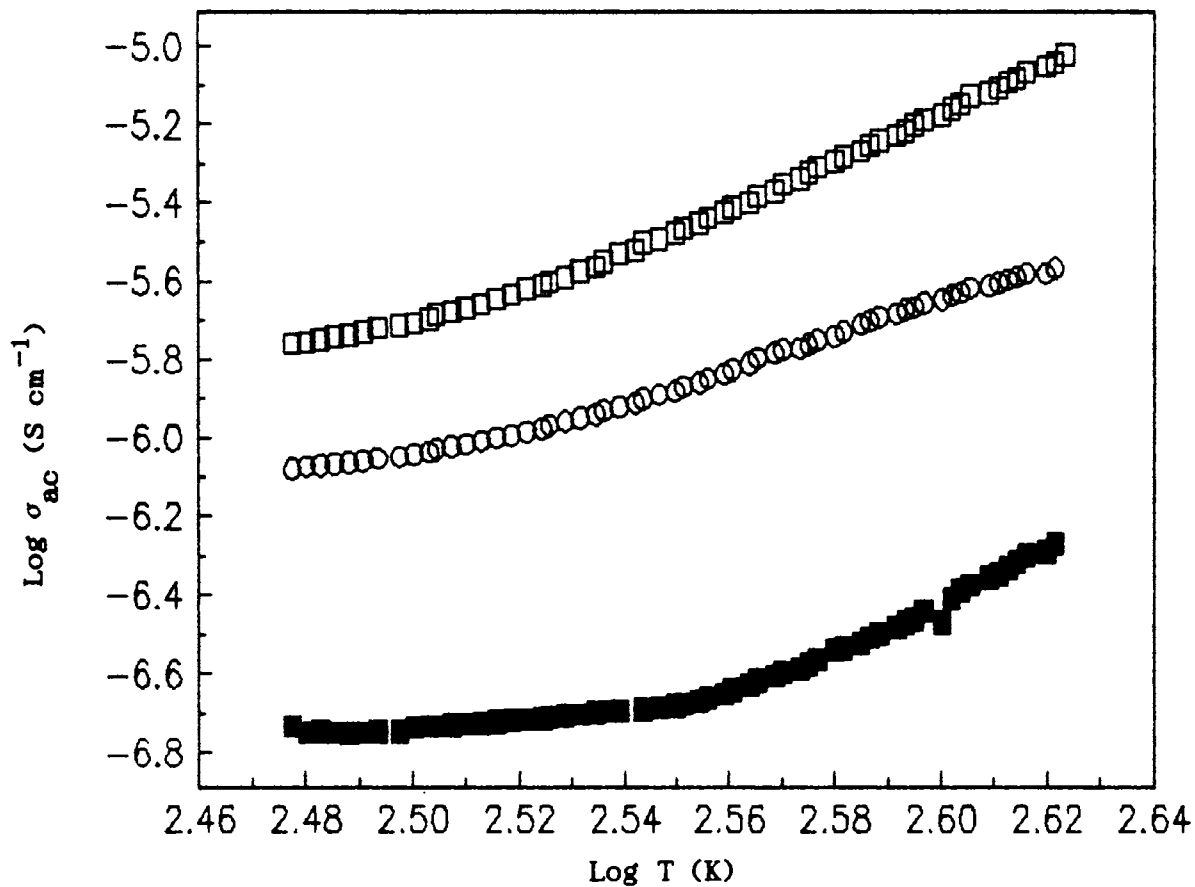●   VONc   O   VONcI

Fig.3.6   Plot of log σ_{ac} versus log T   at three different
frequencies of VONc.
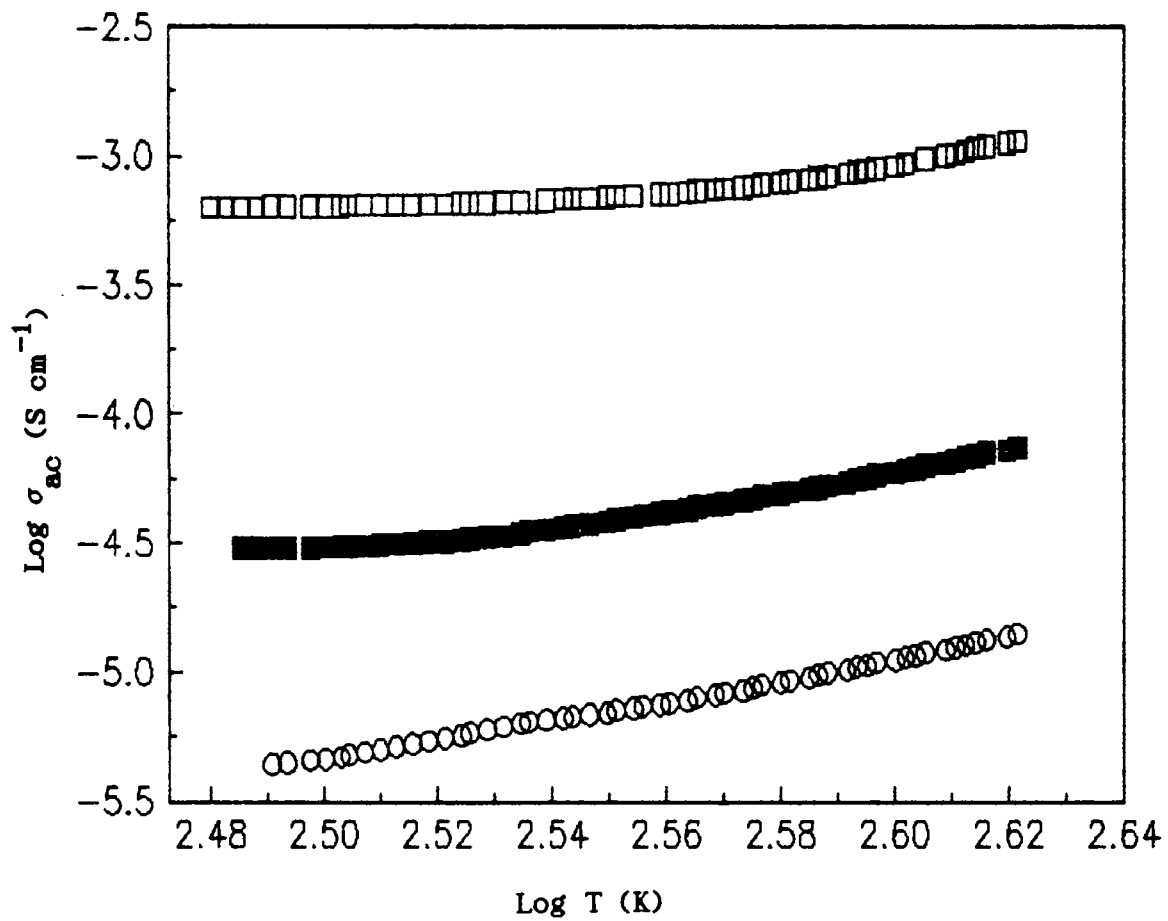
◻   5 MHz   O   1 MHz

■   100 KHz

Fig.3.7   Plot of log σ_{ac} versus log T at three different
frequencies of VONcI.

◻	5 MHz	◼	1 MHz
O	100 KHz		

58

The nonconformity with such a mechanism is evident for pristine sample.

The frequency and temperature dependence of conductivity suggests a mechanism involving excitation of charge carriers from localized states in the gap into localized states in the conduction band edge, with substantial hopping among their localized band states. σ_{ac} of iodine-doped VONc at different temperatures shows that the conductivity at higher frequency is larger than the dc conductivity as expected. This is due to the presence of anomalously large number of sites between which electrons can hop at a greater rate.[29]

The Arrhenius plot for the dc conductivity of ZnNc and iodine-doped ZnNc are presented in the Figure 3.8. The conductivity is enhanced upon doping and the activation energy is also lower in the doped sample.

The temperature dependence of ac conductivity at three different frequencies for ZnNc and ZnNcI shown in Figures 3.9 and 3.10 are characterized by certain features not observed in other naphthalocyanines. In pristine ZnNc temperature dependence of low frequency conductivity shows a broad peak which disappears progressively at higher frequencies. For a polymer such a band is
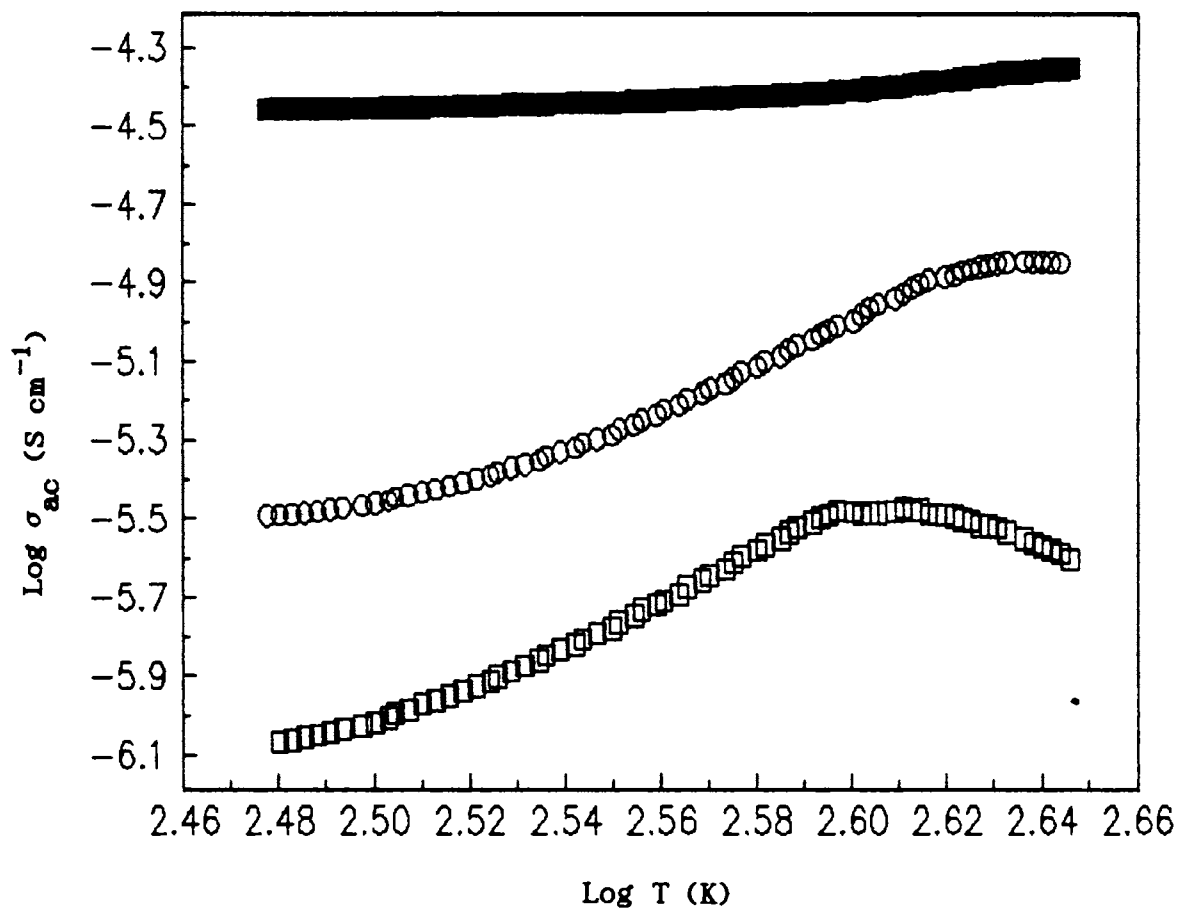
59

Fig.3.8   Log σ_{dc} versus $10^3/T$ plot of pristine and iodine doped
ZnNc

●   ZnNc   O   ZnNcI

Fig.3.9   Plot of log σ_{ac} versus log T at three different
frequencies of ZnNc.

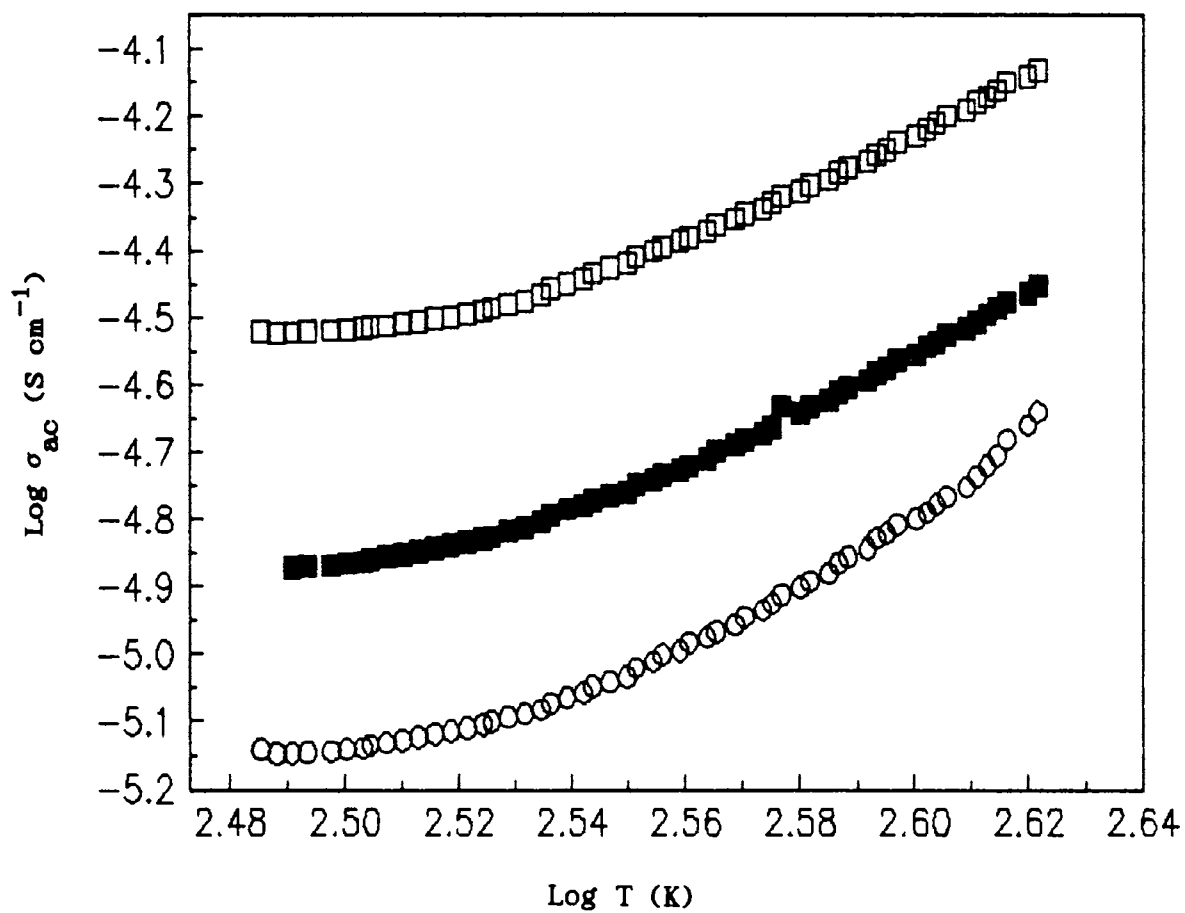■   1 MHz   O   100 kHz

◻   1 kHz

Fig.3.10   Plot of log σ_{ac} versus log T at three different frequencies of ZnNcI.

□   1 MHz   ■   100 kHz

O   1 kHz

usually characteristic of a relaxation phenomenon.[32] That means there is some disorder in the conformations of the quasi-one-dimensional molecule which is progressively relaxed upon increasing the temperature. It is likely that as in phthalocyanines the electrical conductivity in pristine naphthalocyanine is associated with thermal or optical excitation of mobile π-electrons from the valence band containing the highest occupied molecular orbital to the conduction band containing the lowest unoccupied molecular orbital.[33,34]

In doped samples, the relaxation peak disappears indicating that doping has induced not only change in the electronic state, but also a concomitant reorganization of the conformation of the molecule. However the temperature dependence does not fit into the conventional equation describing various modes of hopping.

For a substance to show good conductivity the metal and ligand should be arranged in close communication and in similar crystallographic and electronic environment so that an energetically flat extended pathway exists for electronic charge movement.[35] Also the metal-ligand complex must adopt a "partial oxidation state". By analogy with other MNcs reported it is reasonable to think that in iodine-doped ZnNc, there are stacks of ZnNc units and parallel chains of I_3^- counterions with a disorder

among the latter chains. The partial oxidation of the molecular stack enhances the charge mobility and hence the electrical conductivity is much higher in doped samples.

The temperature dependence of σ_{dc} for pristine and doped $Eu(Nc)_2$ is shown in Figure 3.11. $Eu(Nc)_2$ shows a higher electrical conductivity than the monophthalocyanines studied because of the increased number of conjugated π-electrons in the dinaphthalocyanine ring. Even at low temperature, there is a temperature dependence which becomes considerable at higher temperature. In the doped sample, the conductivity is enhanced, but the order of increase is much less compared to other naphthalocyanines. In order to compliment this information the dc conductivity was plotted in the temperature range 300 K to 420 K (Figure 3.12).

The temperature dependence of ac conductivity is not linear, but depends on frequency as well as temperature (Figures 3.13 and 3.14). This indicates a nonspecific thermally activated hopping process. The flattened 'S' shaped temperature dependence curve becomes almost straightened for the iodinated sample. This also points to the fact that the electronic state in the material has been modified by doping.
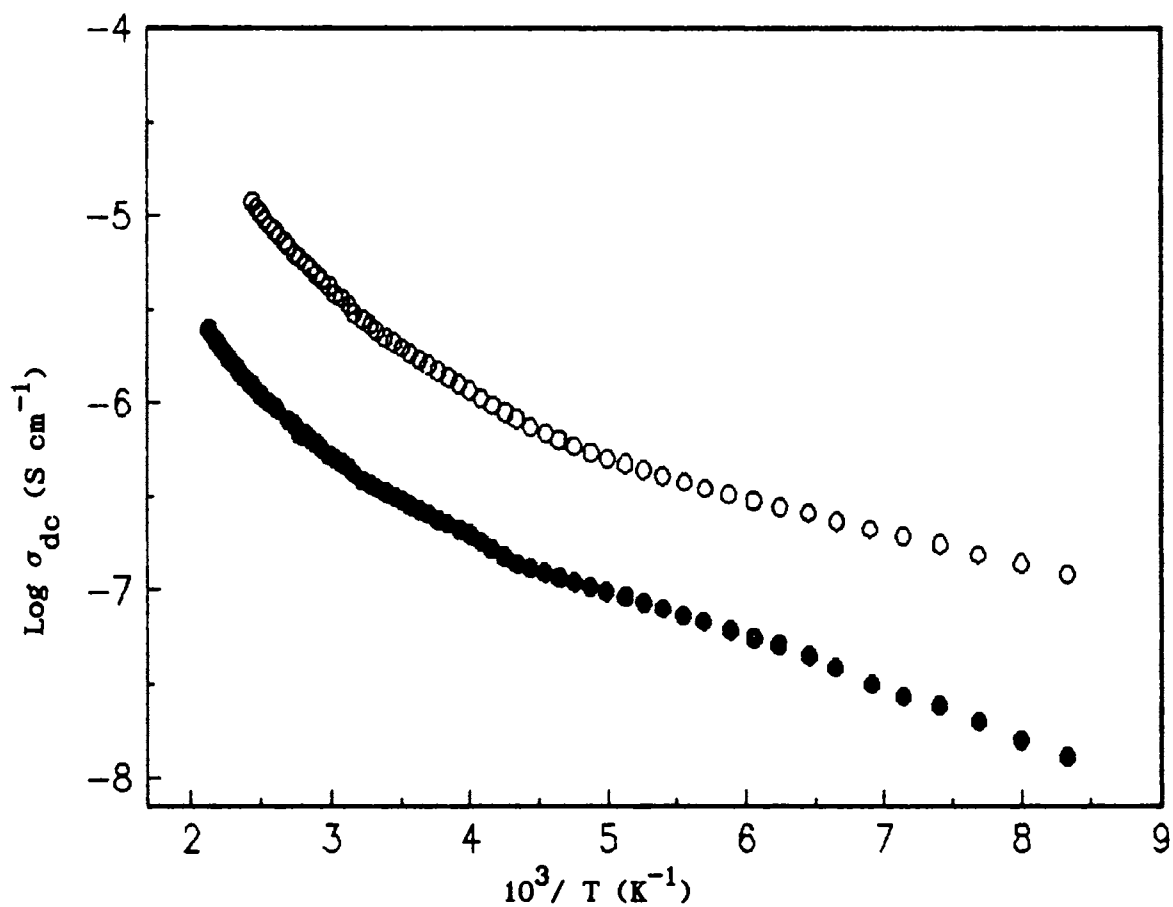
Fig.3.11   Log σ_{dc} versus $10^3/T$ plot of pristine and iodine doped Eu(Nc)$_2$
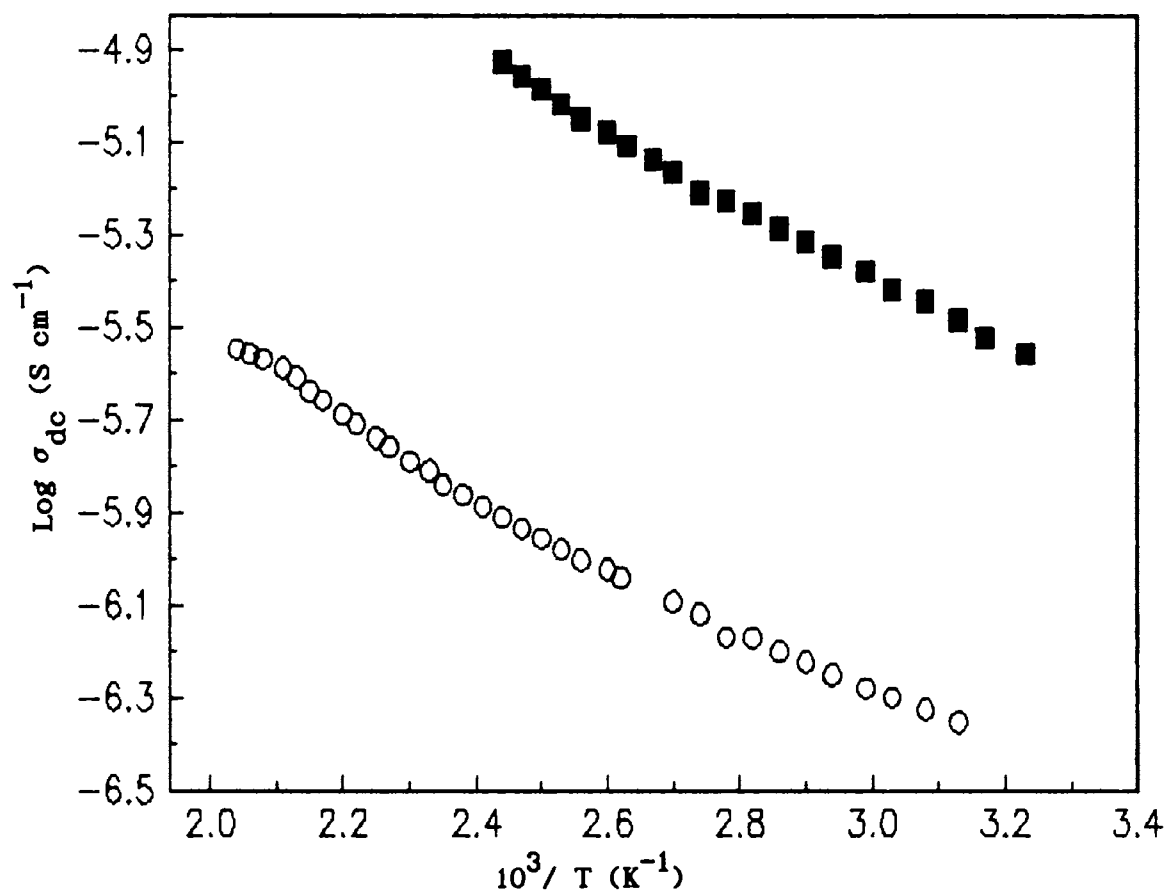
●   Eu(Nc)$_2$ O   Eu(Nc)$_2$I

Fig.3.12   Log σ_{dc} versus $10^3/T$ plot of pristine and iodine doped Eu(Nc)$_2$ from 300 K to 450 K.

O   Eu(Nc)$_2$ ◆   Eu(Nc)$_2$I

Fig.3.13   Plot of log σ_{ac} versus $10^3/T$ at three different frequencies of $Eu(Nc)_2$
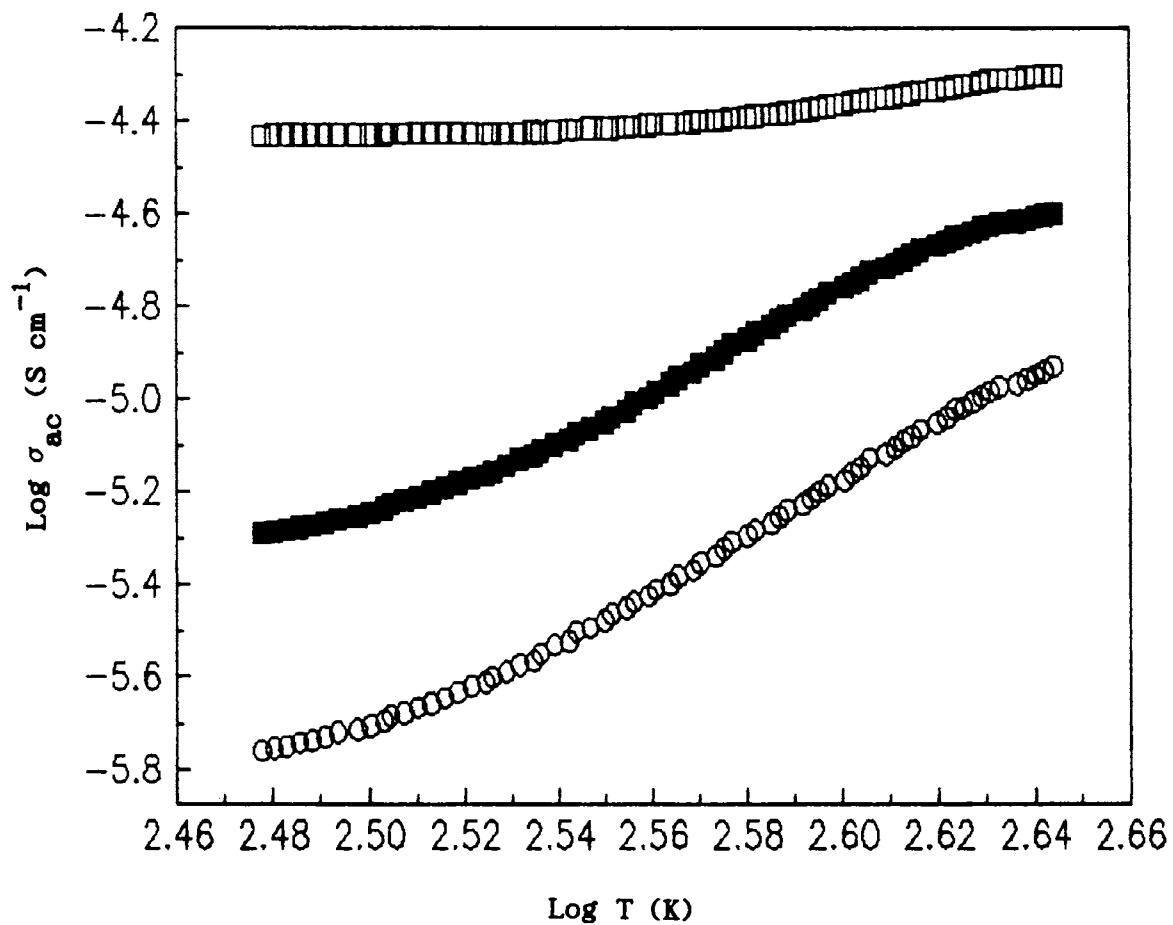
☐   1 MHz   ■   100 kHz

O   1 kHz

67

Fig.3.14　Plot of log σ_{ac} versus log T at three different frequencies of $Eu(Nc)_2I$

☐　5 MHz　　　　　O　　1 MHz

■　100 kHz

The temperature dependence of σ_{ac} may also be due to the thermal activation of charge carriers from localized states in the gap to localized states in the valence or conduction band.[31] At higher frequency (1 MHz) there is not much temperature dependence of conductivity. This effect is not observed in any of the mononaphthalocyanines.

The Arrhenius plots for the temperature dependence of σ_{dc} for pristine and iodine-doped $Eu(Pc)_2$ are shown in Figure 3.15. Thermally activated mechanism becomes very prominent at higher temperature, the activation energies in the two temperature ranges for these samples are given in Table 3.1.

Table 3.1 Activation energies for pristine and iodine-doped europium diphthalocyanine

Samples	Temperature Range (K)	Ea (eV)
$Eu(Pc)_2$	210-330	0.12
	350-500	0.21
$Eu(Pc)_2I$	230-320	0.10
	330-420	0.19
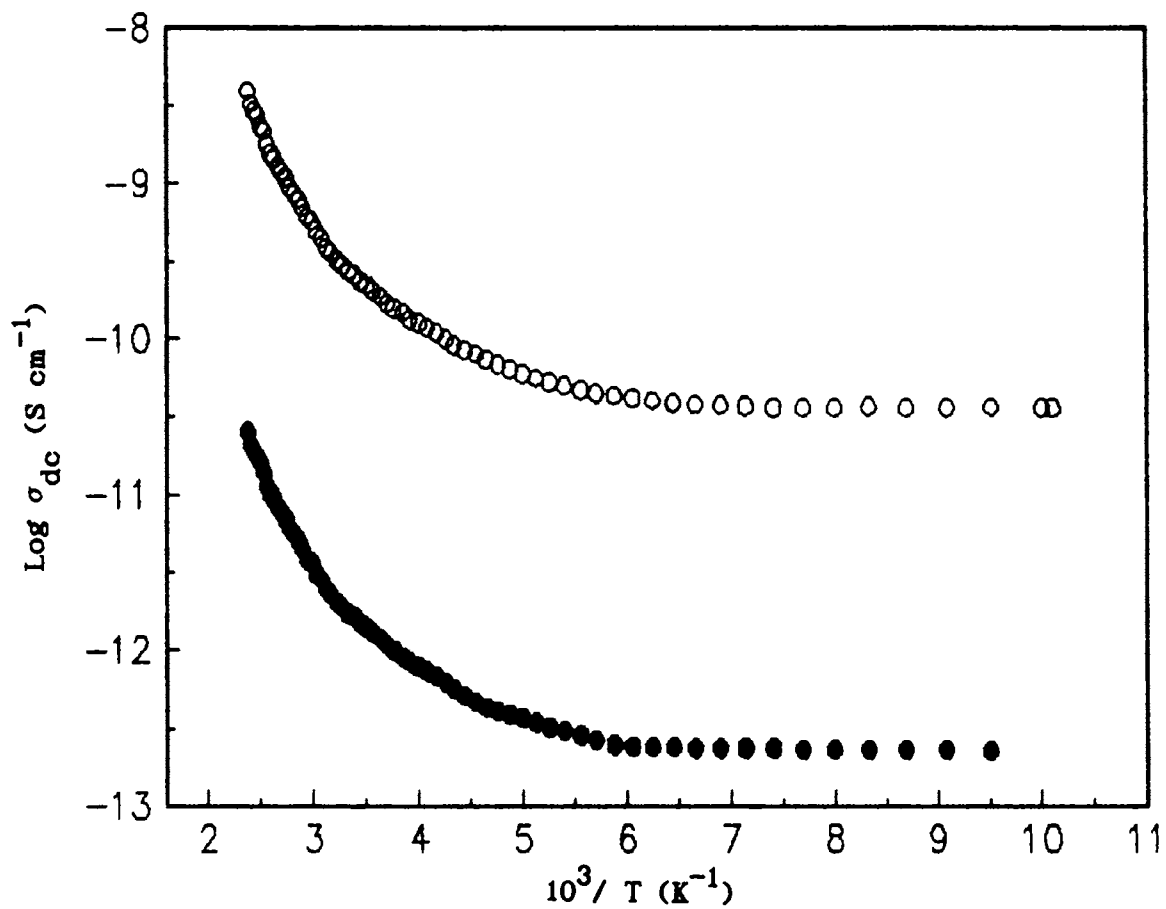
Fig.3.15 Log σ_{dc} versus $10^3/T$ plot of pristine and iodine doped $Eu(Pc)_2$
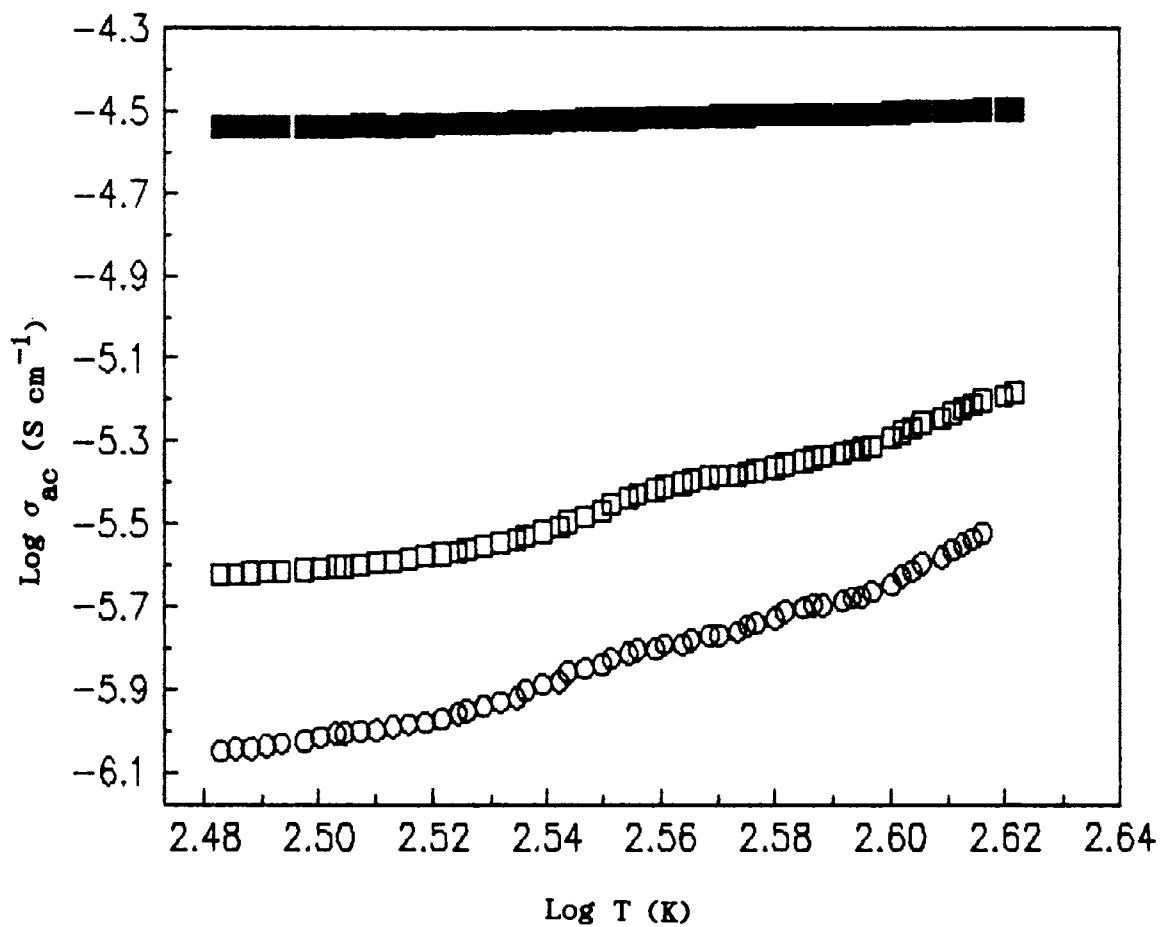
● $Eu(Pc)_2$ O $Eu(Pc)_2I$

70

Fig.3.16   Plot of log σ_{ac} versus log T at three different frequencies of Eu(Pc)$_2$

■   1 MHz   ◻   100 kHz

O   1 kHz
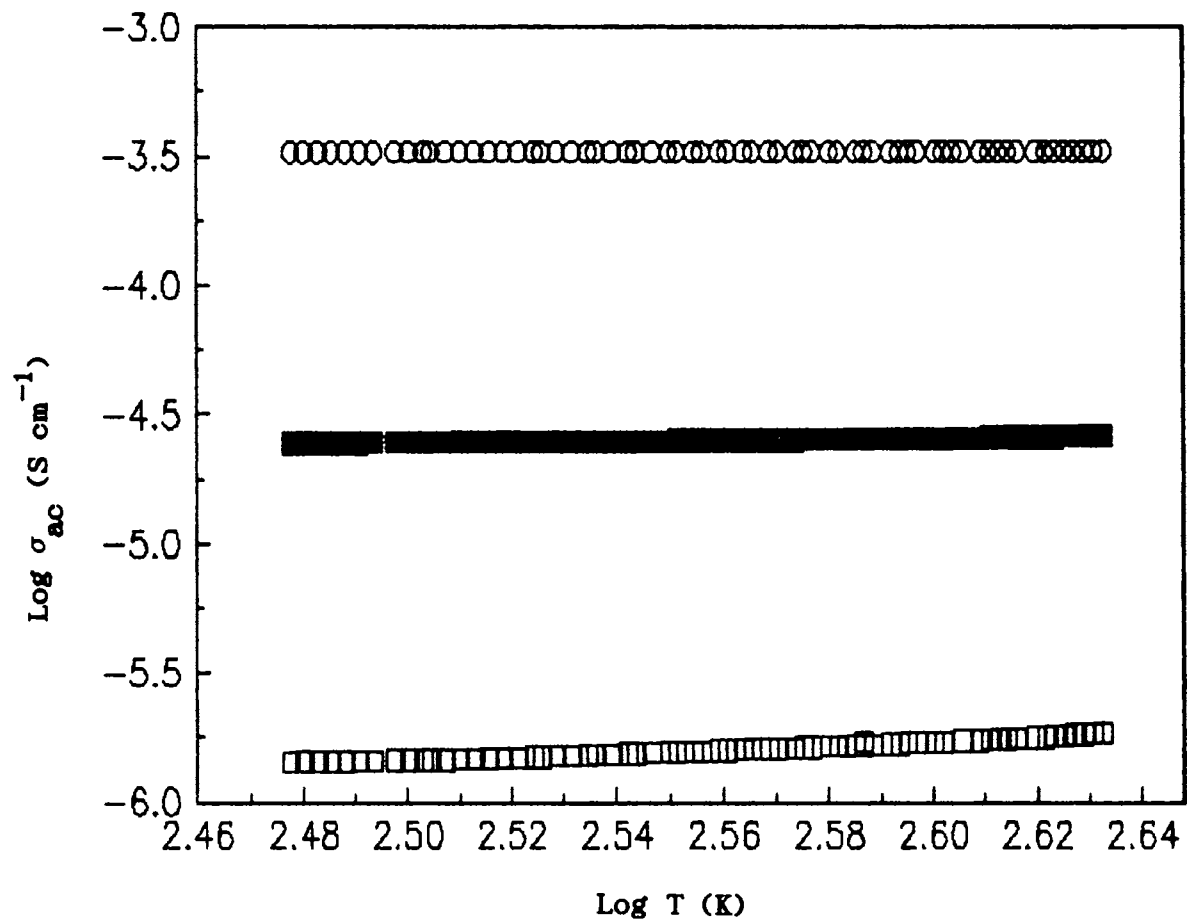
Fig.3.17 Plot of log σ_{ac} versus log T at three different
frequencies of $Eu(Pc)_2I$

O   5 MHz   ■   1 MHz

□   100 kHz

The diphthalocyanine shows conductivity nearly three orders of magnitude lower than that of dinaphthalocyanine. This may be due to the lower π-electron conjugation in diphthalocyanine ring.

The ac conductivity of $Eu(Pc)_2$ has a moderate temperature dependence especially in the lower frequency range upon doping. (Figures 3.16 and 3.17) This pattern changes rapidly and looses its temperature dependence. At the same time, the conductivity has dependence on frequency. This behaviour is very typical of a composite of metal and insulator. The nature of this metal-insulator form is peculiar to $Eu(Pc)_2$ alone compared to other MPcs reported in the literature.

REFERENCES

1. Vartanyan, A.T. *Zn. Fiz. Kleimei.* 1948, 2, 769.

2. Vartanyan, A.T.; Karpovich, I.A. *Dan SSSR* 1956, 111, 561.

3. Vartanyan, A.T. *DAN SSSR, Sesia fiz.* 1956, 1541.

4. Vartanyan, A.T. *DAN SSSR,* 1963, 153, 70.

5. Schramm, C.J.; Scringe, R.P.; Stojkovic, D.R.; Hoffmann, B.M.; Ibers, J. A.; Marks, T. J. *J. Am. Chem. Soc.* 1980, 102, 6702.

6. Misurkin, I.A.; Techougreef, A.L. *J. Chem. Phys.* 1994, 100(3), 2223.

7. Thompson, J.A.; Musata, K.; Miller, D.C.; Stanton, J.L.; Broderick, W.E.; Hoffmann, B.M.; Ibers, J.A. *J. Inorg. Chem.* 1993, 32, 3546.

8. Bufler, J.; Abraham, M.; Bouvet, M.; Simon, J.; Gopel, W. *J. Chem. Phys.* 1991, 95(11), 8459.

9. Fahi, M.R.; Fujimoto, H.; Dann, A.J.; Hoshi, H.; Inokuchi, H.; Maryuama, T.; Willis, M.R. *Phys. Scr.* 1990, 41, 550.

10. Eley, D.D.; Parfitt, G.D. *Trans. Faraday. Soc.* 1955, 51, 1529.

11. Elvidge, J.A.; Linstead, R P.; *J. Chem. Soc.* 1955, 3536.

12. Simon, J.; Andre, J. J. *Molecular Semiconductors,* Springer-Verlag, New York 1985.

13. Yurlova, G.A. *Zh. Obsch. Khim.* 1971, 41, 1325.

14. Wachawek, W.; Zabkowska, M. *Phys. Stat. Solidi* 1980, A60, K17.

15. Gudkov, J.D.; Kozlenkova, N.I.; Yuslova, G.A. *Soviet Physics - Solid State* 1969, 11, 1203.

16. Shimura, M.; Takashi, K.; Shigeki, O.; Yukio, S.; *Hejomen Gijiutsu* 1989, 40(10), 1112.

17. Gretz, R. D.; *Rev. Sci. Instrumen.* 1967, 38, 112.

18. Kopane, V.; Shubin, V.E. *Instrumen. Exp. Tech.* 1976, 19, 1228.

19. Chaudhary, R.K.; Kishore, L. *Cryogenics.* 1977, 17, 419.

20. Abachi, H.; Molenat, J; Malbrunot, P. *J. Phys. E: Sci. Instrumen.* 1979, 12, 706.

21. Gobrecht, H.; Hoffmann, D. *J. Phys. Chem. Solids* 1966, 27, 509.

22. Kaplan, M.L.; Lovinger, A.J.; Reents, W.D. JR; Schmidt, P.H. *Mol. Cryst. Liq. Cryst.* 1984, 112, 345.

23. Petersen, J.L.; Schramm, C.S.; Stjakovic, D.R.; Hoffmann, B.B.; Marks, T.J. *J .Am. Chem. Soc.* 1977, 99, 286.

24. Schramm, C.S.; Stojakovic, D.R.; Hoffmann, B.M.; Marks, T.J. *Science* 1978, 200, 47.

25. Marks, T.J. *Science* 1985, 227, 881.

26. Marks, T.J.; Ibers, J.A. *J. Am. Chem. Soc.* 1975, 97, 3545.

27. Keller, H.J.; Seibold, K.J. *Am. Chem. Soc.* 1971, 93, 1309.

28. Grant, P.M.; Kroumbi, M. *Solid State Commun.* 1980, 36, 291.

29. Nagels, P. *Top. Appl. Phys.* 1979, 36, 114.

30. Mott, N.F.; Davis, E.A. " *Electronic Processes in Non-crystalline Materials,*" Clarendon Press, Oxford, 1979.

31. *"Handbook of Conducting Polymers"*, Vol.2, Skotheim, T. A.(Ed.), Marcel Dekker, Inc., 270 Madison Avenue, New York, 1986.

32. Blythe, A.R. *"Electrical Properties of Polymers,"* Cambridge University Press, London, 1979.

33. Eley, D.D.; Parafitt, G.D., *Trans. Farady Soc.* 1955, 51, 1529.

34. Elvidge, J.A.; Linstead, R.P., *J. Chem. Soc.* 1955, 3536.

35. Emin, D.; Ngai, K.L. *J. Phys. Paris* 1983, 44, C 3-471.

CHAPTER IV

PHOTOACOUSTIC STUDIES ON METAL PHTHALOCYANINES AND NAPHTHALOCYANINES

Abstract

Photoacoustic technique is a recently evolved non-destructive method for probing the thermal properties of the materials. Naphthalocyanines which absorb in the near-ir region have been projected as useful materials for optical data recording. In this context, the thermal diffusivity of these materials is an important engineering property. The thermal diffusivity of naphthalocyanines and phthalocyanines were evaluated by photoacoustic technique and the details are presented in this chapter.

4.1 INTRODUCTION

In order to overcome the limitations of conventional optical methods for the study of optically opaque and weakly absorbing materials, a number of novel optical techniques have been developed during the past few years. Photoacoustic spectroscopy (PAS) and Optical Beam Deflection (OBD) techniques are two such versatile techniques. The fundamental difference between these methods and conventional techniques is that, the interaction of the radiation with the material is evaluated not by the subsequent detection and analysis of the probe beam, but by a direct measure of the energy absorbed by the material and its transduction. These techniques are advantageous in the investigation of metal phthalocyanines and naphthalocyanines which have high optical absorptivity and are insoluble in most of the common organic solvents.

The photoacoustic (PA) signal can be generated either by direct or by indirect methods.[1-5] The acoustic waves are produced in the sample itself for direct PA generation and they are transfered to the coupling medium adjacent to the sample for indirect PA generation. This may be by heat leakage and/or acoustic transmission from the sample. The photoacoustic generation is achieved by continuous wave (CW) mode where the excitation beam is modulated and the signal is analyzed in the

frequency domain i.e., the measurement of amplitude and phase of that signal.

For photoacoustic measurement, the sample is placed in a closed cell or chamber. The solid sample occupies only a small region of the chamber and the remaining region is filled with a non absorbing gas such as air. A sensitive microphone is placed inside the chamber to detect even small pressure variation inside the chamber. A chopped monochromatic radiation is used to illuminate the sample to be studied.

The sample absorbs the incident radiation and the internal energy levels within the sample are excited. On de-excitation, all or part of the absorbed energy is converted into heat energy through nonradiative de-excitation process. The heat energy appears as kinetic energy in the case of gas molecules while it appears as vibrational energy of ions in solids. The heat generated within the sample will be modulated as a result of the modulation of incident radiation. The periodic heating of the sample due to the absorption of optical energy results in a periodic heat flow from the sample to the coupling gas. Hence pressure and volume changes are produced in the gas which drive the microphone.

The advantages of PAS is that the PA signal is generated only after the absorption of optical signal, the light that is transmitted or elastically scattered by the sample does not interfere with PA measurements. Added advantage of this technique is that the absorption spectra of optically opaque samples are obtained since the method does not depend on the detection of radiation. The PA effect results from a radiationless energy conversion process and is therefore complementary to radiative and photochemical processes.[6-11]

4.2 THEORY

4.2.1 Photoacoustic technique

According to the one dimensional model of Rosencwaig and Gersho,[1,3] the pressure variation δP at the front surface of an optically thick sample irradiated with a chopped beam of monochromatic radiation depends on the thermal diffusivity α_s of the sample. The theoretical expression of δP may be written as

$$\delta P = X \ Y \qquad \text{————————(4.1)}$$

In the above relation

$$X = \left[1 + g\ \frac{h^+ + h^-}{h^+ + h^-}\right]^{-1} \left[\frac{h^+ + h^-}{h^+ - h^-} + g\right]\ \frac{1}{\sigma_s l_s^2}$$

$$\text{------------(4.2)}$$

where

$$h^+ = \exp\ (\sigma_s\ l_s)$$

$$h^- = \exp\ -\ (\sigma_s\ l_s)$$

$$\sigma_s = (\ 1 + j\ )\ (\ \pi f/\ \alpha_s)^{1/2} \qquad \text{------------(4.3)}$$

$$g = \frac{e_b}{e_s} = \frac{k_b}{k_s}(\alpha_s\ /\ \alpha_b)^{1/2}, \quad \text{the ratio between the}$$

effusivities $\left[e= \left(\dfrac{k}{\rho C}\right)\right]^{1/2}$ of the backing (e_b) and the sample (e_s) and

$$Y = \frac{P_0\ \gamma\ W_a\ l_s^2\ (\alpha_g)^{1/2}}{2\ l_g\ T_0\ k_s\ (\alpha_s)^{1/2}} \qquad \text{--------(4.4)}$$

Here l, k, ρ and C are length in cm, thermal conductivity in cal $g\ s^{-1}\ K^{-1}$, mass density in $g\ cm^{-3}$, specific heat capacity in cal $g^{-1}\ K^{-1}$, and the subscripts g, s and b refer to the gas (air), sample and backing material respectively. P_0 and T_0 are the ambient pressure and temperature of the gas, γ is the specific heat

ratio for air, W_a is the absorbed power of light. The term X depends on the modulation frequency f through the product $\sigma_s \, l_s$, which can be written as

$$\sigma_s \, l_s = (\, 1 \, + \, j \,) \, (\pi f/f_c)^{1/2}$$

where the characteristic frequency f_c is obtained from equations 4.3 and 4.5 as $f_c = \alpha_s/l_s^2$. The f_c can be found out by plotting log A against log f where A is the amplitude of the PA signal (which is directly proportional to δP). When chopping frequency f becomes equal to f_c a change in slope occurs in the above plot.

4.2.2   Thermal diffusivity

Thermal diffusivity is important as it determines the rate of periodic or transient heat propagation through a medium. The thermal diffusivity requires the measurement of the time for a thermal disturbance to propagate through a known distance in the medium.

Transient heat flow method[12] and periodic heat flow method[13] are the two techniques which are commonly used to determine the thermal diffusivities. An addition or removal of thermal energy from the sample induces a transitory temperature change and thermal

82

diffusivity is determined by measuring temperature as a function of time at one or more points along the sample in the transitory heat flow method. In the periodic heat flow method, the thermal energy supplied to the sample is modulated at a fixed period. Hence the temperature at all points in the sample vary with the same period and thermal diffusivity is determined from the measurement of amplitude and phase of thermal wave in the sample. The photoacoustic technique belongs to the periodic heat flow method.

Thermal diffusivity is related to the thermal conductivity by the relationship

$$\alpha = \frac{K}{\rho c}$$

where
α – thermal diffusivity ($cm^2 s^{-1}$)

K – thermal conductivity (cal $cm^{-1} s^{-1} K^{-1}$)

ρ – density (g cm^{-3})

c – specific heat capacity (cal $g^{-1} K^{-1}$)

4.3 EXPERIMENTAL

4.3.1   Sample preparation

For thermal diffusivity measurements, the naphthalocyanine and phthalocyanine samples were finely powdered and pressed (2000 kg cm^{-2}) to pellets of diameter 5 mm and thickness 0.5 mm to 0.8 mm. The naphthalocyanine and phthalocyanine samples of appropriate thickness were taken for the measurement so that the characteristic frequency at which a transition from thermally thin to thermally thick regime take place at that thickness as the chopping frequency is varied from 20 Hz to 100 Hz.

4.3.2   Experimental set-up

The essential requirements of a PA measurements are a radiation source, frequency modulator, PA cell consisting of the sample holders and acoustic transducer and a signal processing unit.

The schematic diagram of the experimental set-up used for PA measurement is shown in the Figure 4.1. It consists of (i) a pump source (ii) an electromechanical chopper (iii) PA cell and (iv) a lock-in amplifier.
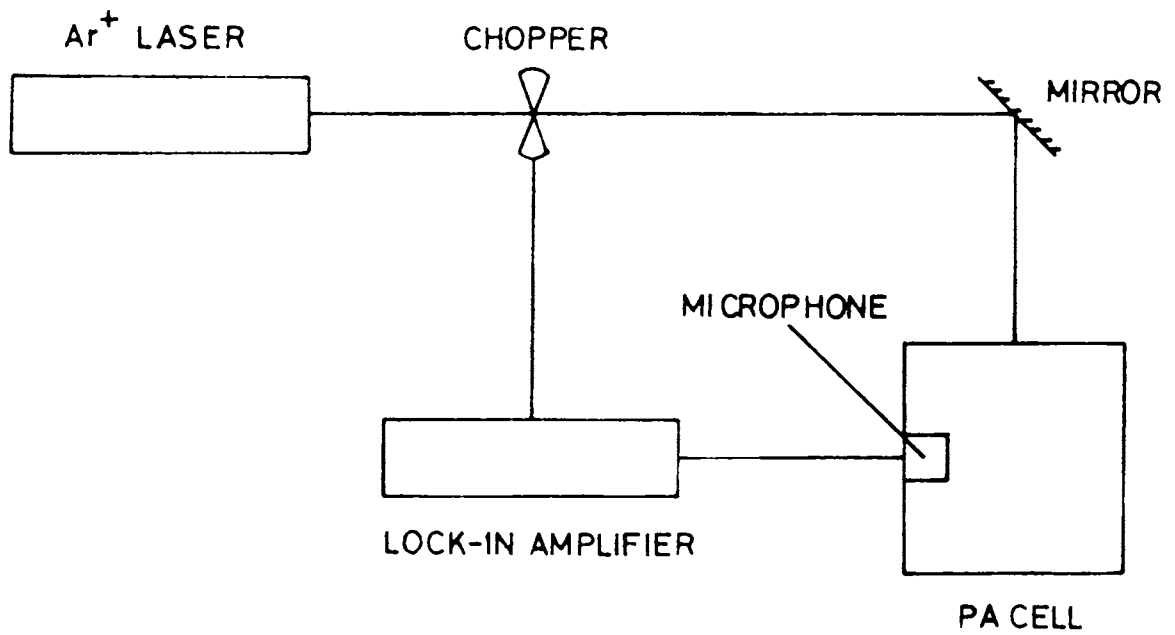
84

Fig.4.1 Schematic diagram of the experimental set-up used for photoacoustic measurement.

The pump source used in this study is a continuous wave Ar^+ laser (Liconix 5000 series) at a power level of 26 mW. The excitation wave length used is 488nm. In order to obtain acoustic signal in the PA cell, the laser beam was modulated before irradiation of the sample. An electromechanical chopper (Stanford Research System, INC, Model SR 540) was used for modulating the laser beam.

The PA cell used had a cylindrical cavity of 5 mm length and 10 mm diameter made in a solid block of stainless steel. One end of the bore was closed by a glass window and the sample was placed on the other side and closed air-tight. The PA signal was detected using a Knowel's 1753 electret microphone kept very close to the sample compartment in a separate port. The glass window and the microphone were sealed with o-rings and air at atmospheric pressure was the coupling medium. The output from the microphone was fed to a lock-in amplifier (EG&G Model 5208) through a BNC connector.

The lock-in amplifier uses phase sensitive detection to single out the component of the signal at the reference frequency and phase. Noise at frequencies other than the reference frequency are rejected and does not affect the results.

The experimental procedure is standardised by determining the thermal diffusivity of a sample of copper with a value of 1.16 cm^2s^{-1}. The result obtained is in close agreement with the reported value (1.14 cm^2s^{-1}). Hence the method is extended to samples whose thermal diffusivities have to be evaluated.

4.4 RESULTS AND DISCUSSION

The amplitude of the PA signal was measured as a function of the chopping frequency in the range 20 Hz to 100 Hz for metal free, zinc and vanadyl naphthalocyanines and europium naphthalocyanine and phthalocyanine. Measurements were carried out with their iodine doped samples also. The log amplitude vs log frequency plots obtained for these samples and their iodine doped forms are given in the Figures 4.2 to 4.6. The characteristic frequency (frequency at which a sudden slope change occurs) for each of these substances was obtained from these graphs. The characteristic frequency of the samples were evaluated and used to calculate thermal diffusivity (Table 4.1).

The magnitude of the thermal diffusivity values obtained from these samples are comparable with that of other phthalocyanines and inorganic semiconductors like germanium. From the results

87
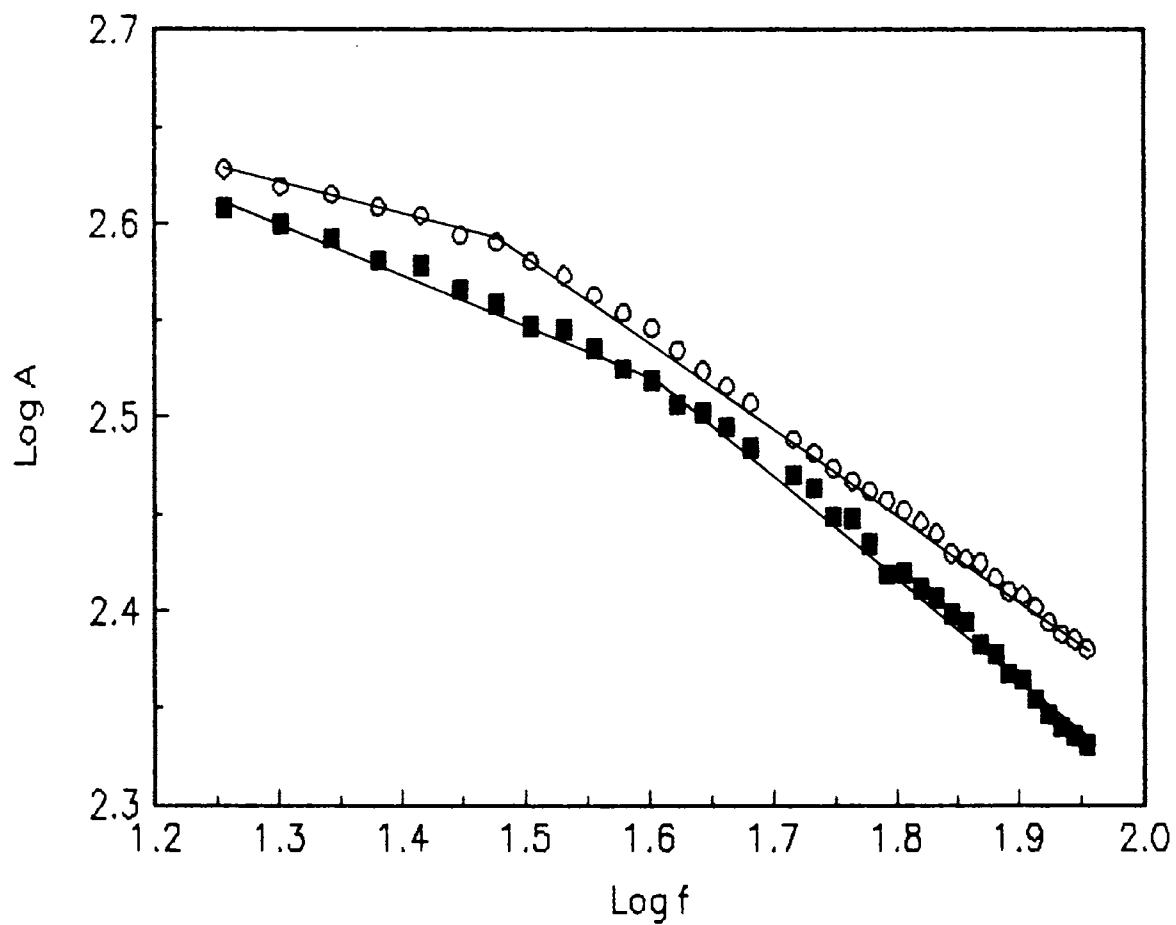
Fig.4.2   Log A versus log f plot of pristine and iodine doped metal free naphthalocyanines.

O H_2Nc ■ H_2NcI

Fig.4.3   Log A versus log f plot of pristine and iodine doped
vanadyl naphthalocyanine.

O   VONc   ■   VONcI
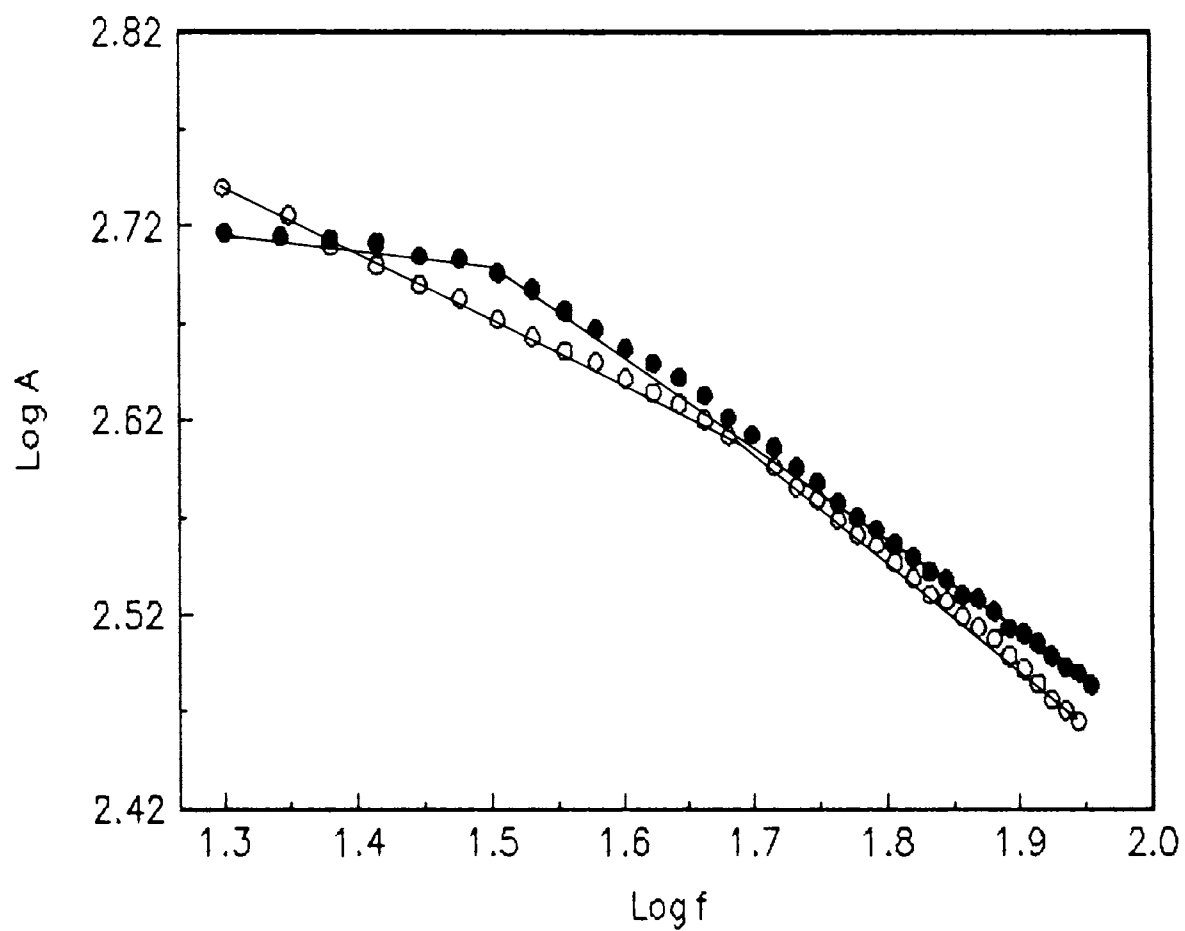
Fig.4.4   Log A versus log f plot of zinc naphthalocyanine in the
pristine and iodine doped forms.

   ●   ZnNc   O   ZnNcI
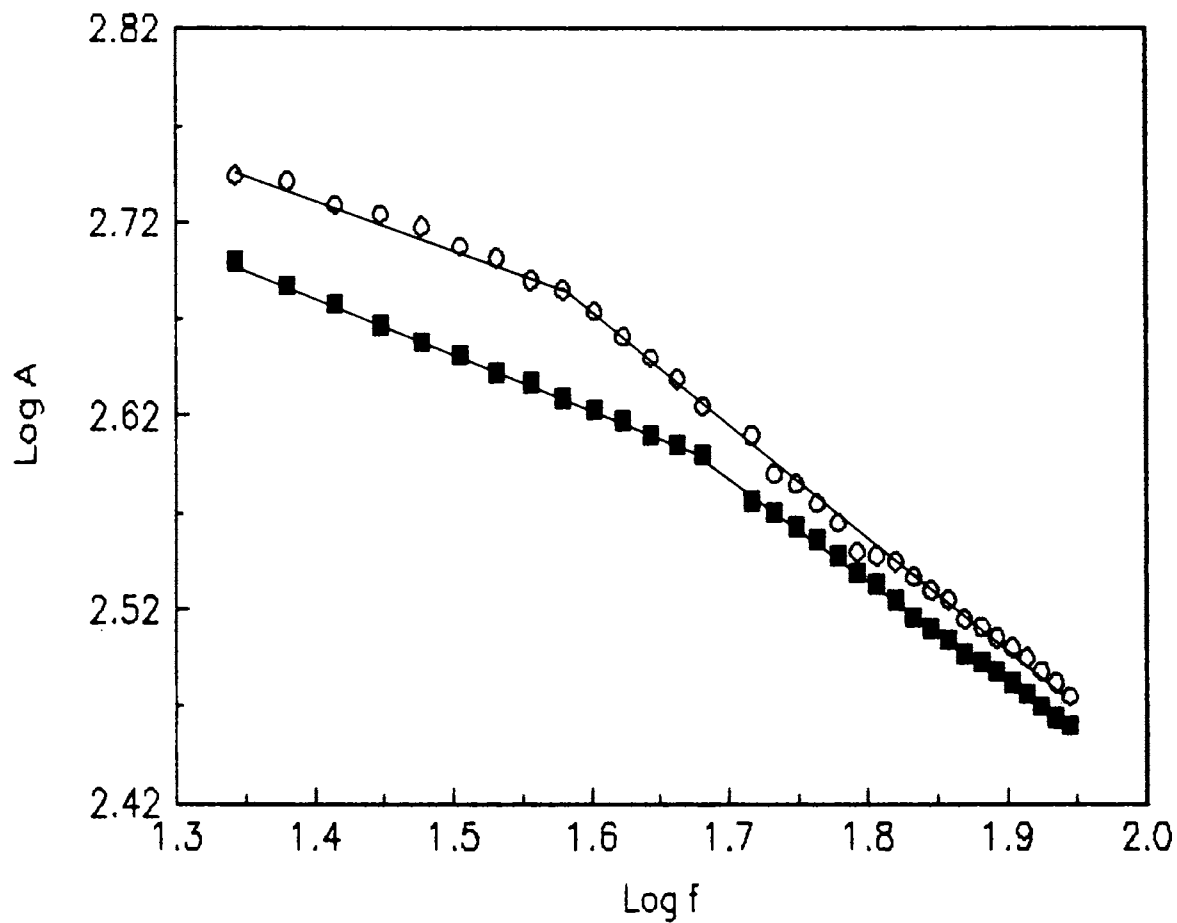
Fig.4.5   Log A versus log f plot of pristine and iodine doped

europium dinaphthalocyanine.

O   Eu(Nc)$_2$ ■   Eu(Nc)$_2$I

91
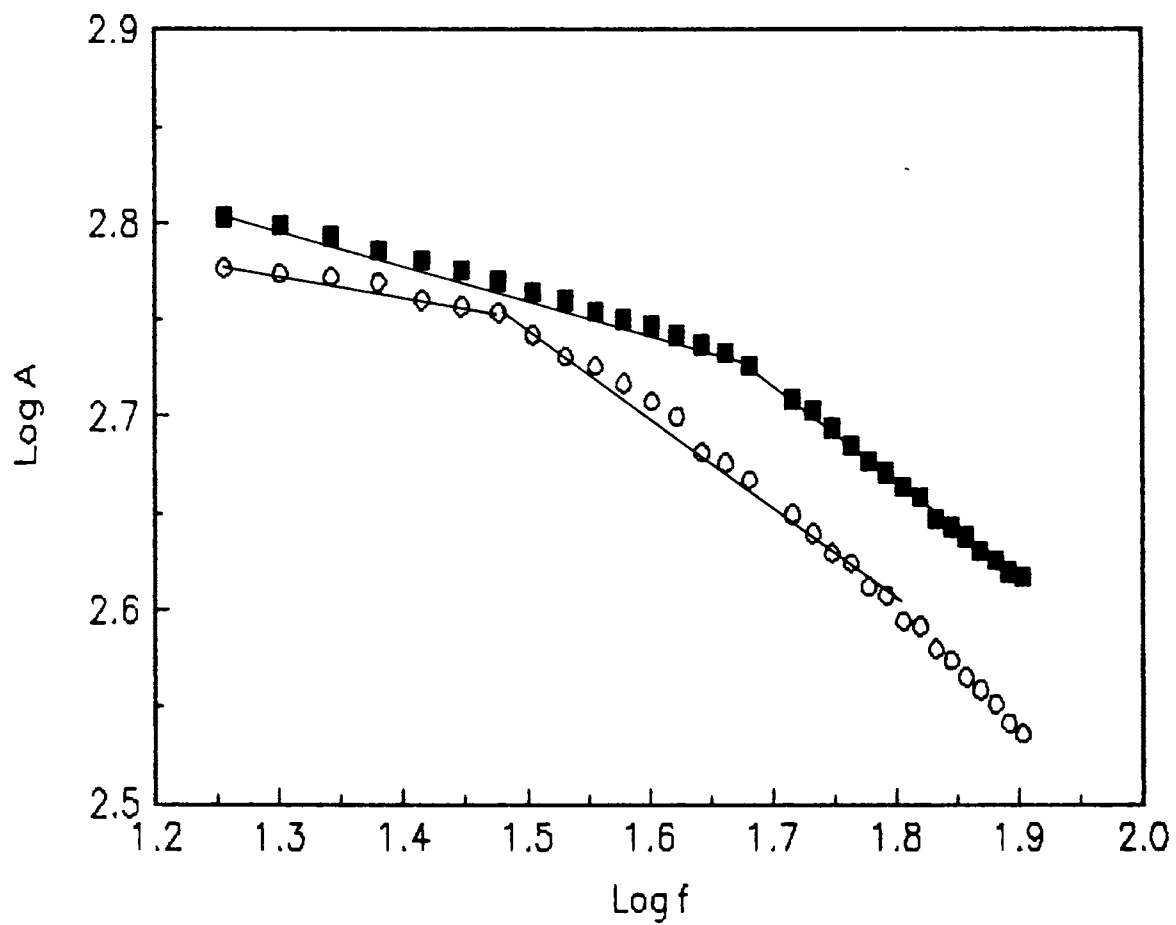
Fig.4.6   Log A versus log f plot of europium diphthalocyanine in
the pristine and iodine doped forms.

O   Eu(Pc)$_2$ ■   Eu(Pc)$_2$I

Table 4.1 Thermal diffusivity values of pristine and iodine doped samples of naphthalocyanines and phthalocyanine.

Sample	Characteristic frequency	Thermal diffusivity cm^2s^{-1}
ZnNc	32.4	0.10
ZnNcI	46.8	0.15
VONc	43.7	0.26
H_2Nc	29.9	0.13
H_2Nc1	39.8	0.17
$Eu(Nc)_2$	37.6	0.20
$Eu(Nc)_2I$	47.3	0.23
$Eu(Pc)_2$	29.9	0.12
$Eu(Pc)_2I$	48.4	0.14

presented in the Table 4.1, it can be seen that the thermal diffusivity values of iodine doped samples are substantially higher than that of pristine samples. It must be noted here that a very large increase in electrical conductivity values has been observed in these samples on doping with iodine. This points to the significant role of electronic carriers in contributing to the thermal conduction mechanism in organic semiconductors like naphthalocyanine and phthalocyanine.

REFERENCES

1. Attlar, A. *Appl. Opt.* 1980, 19, 3204.

2. Tam, A.C.; Coafal, A.*J. Phys.* 1983, C6,9.

3. Mc. Donald; Wetsel, Jr. J. *Appl. Phys.* 1978, 49, 2313.

4   Monchalin, J.P.; Bertrand, L.; Rousset, G.; Flepoutre, F. *J. Appl. Phys.* 1984, 56, 190.

5. Somasundaram, T.; Ganguly, P. *J. Phys. (Paris) Coloq.* 1983, C6, 239.

6. Tom, A.C. *Appl. Phys. Lett.* 1980, 37, 978.

7. Thielemann, S.; Newmann, H. *Phys. Stat. Solidi* (a) 1980, 61, K 123.

8. Kiskbright, G. F.; Miller, R. M. *Analyst,* 1982, 107, 798.

9. Rosenewaig, A.; Buss, G. *Appl. Phys. Lett.* 1980, 36, 725.

10. Wong, T.H.; Thomas, R.L.; Hawkins, G.F. *Appl. Phys. Lett.* 1978, 32, 538.

11. Wickramasinghe, Brag, R.L.; Jipson, V.; Quate, C. F.; Salecda, J.R. *Appl. Phys. Lett.* 1978, 932, 33.

12. Parker, W.J.; Jenkins, R.J.; Butler, C.P.; Abdot, G.L. *J. Appl. Phys.* 1961, 32, 1679.

13. Abelis, B.; Cody, G.D.; Beers, D.S. *J. Appl. Phys.* 1960, 31, 1585.

CHAPTER V

THERMAL DIFFUSIVITY MEASUREMENTS ON
METAL PHTHALOCYANINES AND NAPHTHALOCYANINES
BY PHOTOTHERMAL DEFLECTION TECHNIQUE

Abstract

Materials like dyes with high absorptivity are being developed for writing and reading using semiconductor lasers. The writing process is achieved by photothermal pit formation using a moderate intensity laser beam. In this connection, the chemical stability, optical absorptivity, and thermal diffusivity are the critical properties, required to make a decision on the choice of the compound. The thermal diffusivity of these materials were evaluated by optical beam deflection technique. Naphthalocyanines which strongly absorb in the near-ir region falls as a natural selection. The experimental technique and the results are described in this chapter.

5.1   INTRODUCTION

The thermal diffusivity (α) is a critical property for materials used in optical recording applications.[1] This parameter is a measure of the rate of diffusion of heat in a material.

In the conventional method for determining thermal diffusivity, the sample is excited by a heat source and the resulting temperature distribution is determined by suitable temperature sensors. There are two experimental methods to determine thermal diffusitvity depending on whether the heat flow is periodic or transient. For transient excitations a change in the amplitude or the pulse shape of the diffusing heat pulse is determined, while for periodic excitation the pulse shift of thermal wave diffusing across the sample is measured. In both cases the detection is made using thermocouples which are in contact with the sample. This may cause fluctuation in the thermal field to be measured.

Photothermal technique has replaced thermometers for thermal detection. The high sensitivity of the method together with the noncontact generation of a well defined heat source is the major advantage of this method.

5.2 PHOTOTHERMAL DEFLECTION TECHNIQUE

5.2.1 Photothermal effects

Photothermal effects depend on the thermal de-excitation path of excited atoms or molecules.   The heat generated will be a function of numerous parameters related to the sample and the surrounding medium.   Photothermal measurements are ideal for the quantitative evaluation of a number of properties such as (i) thermal diffusivity and effusivity   (ii) charge carrier diffusivity (iii) thermal conductivity (iv) spectroscopic properties like absorption coefficient and (v) geometrical parameters of the sample like thickness and fractal dimensions.

The temperature distribution in a light absorbing sample and in the air nearer to the sample surface has been described   by Mc Donald et al.[2] An increase in temperature of a sample when it is irradiated by a chopped beam can be expressed by the relation

$$\Delta T = \frac{\beta P}{2f\rho c \mu A}$$

β – optical absorption coefficient

P   – the incident laser power

f   – chopping frequency

A   – area of the sample

99
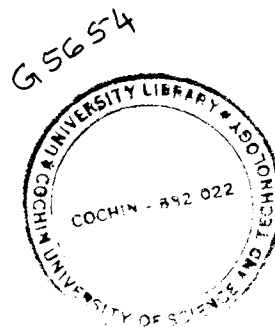
ρ - density of the sample

c   - specific heat of the sample and

μ - thermal diffusion length

The thermal diffusion length is given by the expression

$$\mu \quad = \quad (\alpha/\pi f)^{1/2}$$

where α is the thermal diffusivity of the sample.

In photothermal technique there is absolutely no signal in the absence of an excitation beam and hence termed "zero background". This is in contrast to the conventional techniques in which the measurements are carried out on a beam transmitted or reflected from the sample. Hence by properly optimizing the technique, photothermal technique provides a much improved absorption sensitivity than the conventional methods.[3] It has several advantages like simplicity of experimental set up, easy sample preparation and a wide range of applications. The technique is applicable to a variety of samples such as opaque materials, powders, films and aerosols. Complicating phenomena like quenching, diffusion, recombination etc which are serious limitations of ultra sensitive detection techniques are of very little significance to photothermal technique.
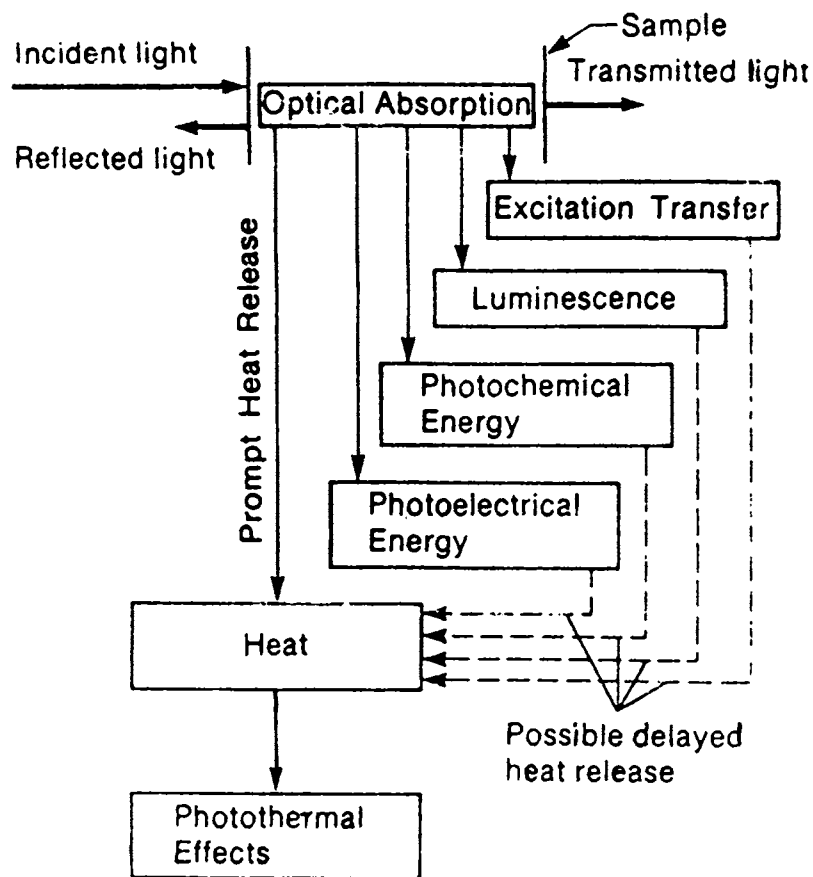
Fig.5.1   Optical   absorption   and   various   possible   de-excitation
paths leading to photothermal effects

5.2.2   Photothermal signal detection

In photothermal technique, a modulated heating beam called pump
beam is incident on the sample surface.   It induces a rise in the
temperature at the sample surface which, in turn, increases the
temperature of the coupling medium (air) immediately adjacent to the
surface due to thermal diffusion.   There are also some other

photothermal effects such as change of refractive index in the sample and in the adjacent medium, formation of acoustic waves, and emission of infrared radiations which take place simultaneously or with time delay. The selection of a suitable photothermal effect for detection depends on the nature of the sample and its environment, the source used and the purpose of measurement.

When detection method is directly applied to the sample it is called direct photothermal effect or to the coupling fluid adjacent to the sample which does not absorb incident light, it is called indirect photothermal effect. The direct photothermal effects offer high sensitivity for weak absorptions whereas indirect photothermal effects are used for opaque, highly scattering and inhomogeneous samples.

5.3   THEORY

Several groups[4-9] have proposed PTD technique for the measurement of thermal diffusivity. The proposed theory is that the probe beam has a transverse offset y, with respect to the pump beam axis, and a   vertical offset z, with   respect to   the sample surface. The schematic of the PTD method showing the two detection methods are shown in Figure 5.2.

The transverse and vertical offsets of probe beam with respect

FOCUSED
EXCITATION
SOURCE

POSITION SENSITIVE
DETECTOR

ϕ_n

φ_t

DIAGRAMMATIC
REPRESENTATION OF
SURFACE TEMPERATURE
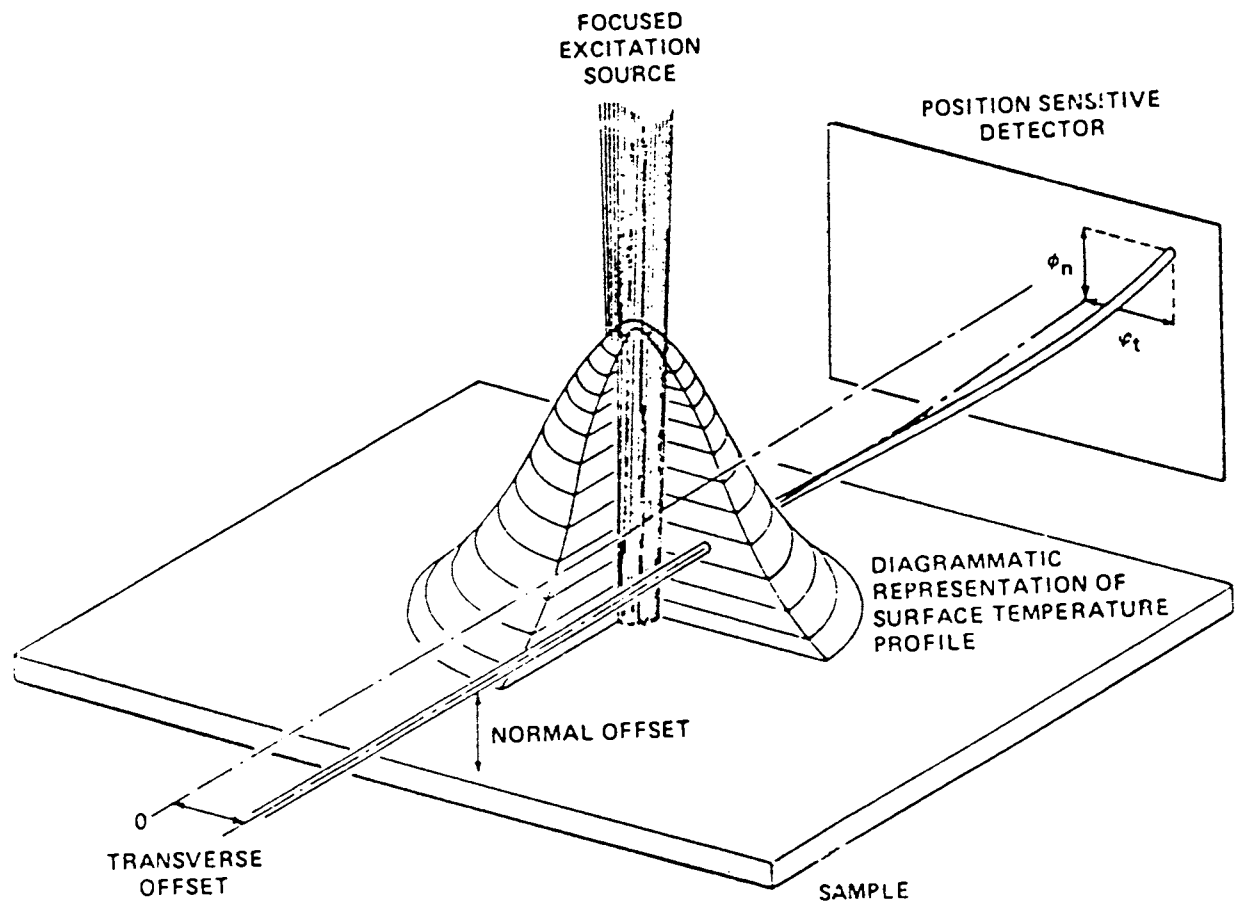PROFILE

NORMAL OFFSET

0

TRANSVERSE
OFFSET

SAMPLE

Fig.5.2   Schematic diagram of the PTD method showing the two
deflection components

to the pump beam axis are y and z respectively. Because of the vectorial structure of the deflection, the transverse (ϕt) and normal components (ϕn) can be estimated as

$$\phi_t = \frac{1}{n} \frac{\partial n}{\partial t} \int_{-\alpha}^{\alpha} \frac{\partial T}{\partial y} \, dx$$

$$\phi_n = \frac{1}{n} \frac{\partial n}{\partial t} \int_{-\alpha}^{\alpha} \frac{\partial T}{\partial z} \, dx$$

where n is the refractive index of the medium and T is the temperature near the heated sample at time t. The terms s and **g** denote solid and gaseous phases respectively.

The total deflection M is

$$M = \left| \phi_n \right|^2 + \left| \phi_t \right|^2$$

$$\text{Since} \left[\frac{\partial n}{\partial T} \right]_s \gg \left[\frac{\partial n}{\partial T} \right]_g, \quad \text{then } \Delta T_s > \Delta T_g$$

Therefore the deflection $\left|\phi_s\right|$ $\gg$ $\left|\phi_g\right|$, which is true for both the normal and transverse components. The term $\Delta T = \dfrac{\partial T}{\partial z}$ which includes the cosine term which makes the deflection symmetrical with respect to the pump sources, whereas the transverse deflection $\Delta T = \dfrac{\partial T}{\partial y}$ includes the sine term making it antisymmetric about the source. Hence, ϕ_t becomes zero and changes phase by 180° at the origin. The ϕ_t dominates over the normal component near the interface along the source while ϕ_n dominates near the interface away from the sources.[10]

When the pump beam is incident on the sample, thermal waves are generated which cause changes in the refractive index thereby producing a gradient within the sample or in the adjacent coupling medium surrounding the sample. A plane thermal wave has the form $\exp(j\omega t - \delta x)$, where $\delta = (1+j)(\omega / 2\alpha)$ and $\omega = 2\pi f$; where f is the chopping frequency. Thermal waves get attenuated rapidly by a factor e^{-1} in a distance called the thermal diffusion length (μ) where $\mu = (2\alpha / \omega)^{1/2}$; and in a distance of one thermal wavelength $\lambda_t = 2(\pi\alpha / f)^{-1/2}$, the amplitude is decreased by a factor $\exp(-2\pi) = 0.002$.

The thermal waves which are produced in the sample at a depth more than λ_t will have little effect on the air and thereby not affecting the photothermal signal. The normal waves reaching the

coupling gas medium are confined to a thin layer adjoining the sample surface.

5.4   APPLICATIONS OF PHOTOTHERMAL DEFLECTION TECHNIQUE

The photothermal deflection (PTD) technique is a versatile, nondestructive technique.   It has numerous applications in spectroscopy, imaging, and studies on laser induced damage and ablation, phase transition, thermodynamic transport properties, gas flow velocity measurements, combustion diagnostics and trace gas analysis.

Thermal properties of different classes of compounds like conducting, insulating, organic, inorganic, crystalline and amorphous samples can be carried out using photothermal deflection technique.   Among the various thermal parameters, thermal diffusivity is the most important one for solid samples, which has been determined by several workers[11,12] by PTD technique.   Thermal diffusivity (α) is related to thermal conductivity (k) of the sample by the relation $\alpha = k/\rho Cp$ where ρ is the density and Cp is the specific heat capacity at constant pressure.

Ramtala[13] has determined the thermal diffusivity of very low diffusivity materials like polymers, plastics etc. in the form of thin foils.   The lower limit of·thermal diffusivity determined by

them was of the order of 10^{-4} cm^2s^{-1} and it agrees well with the values obtained using the flash method.[14] PTD technique has been used for the detection of a large variety of samples including liquid crystals,[15-17] high temperature superconductors[18] and organic semiconductors.[19] It has been observed that anomalous changes in amplitude occur in the signal level near the transition temperature of doped glasses,[20] chalcogenide glasses[21] and semiconductor doped glasses.[22]

5.5   EXPERIMENTAL

In PTD technique, the initial requirements that have to be adequately satisfied are (i) isolation of optical and sample mounts for minimising extraneous vibrations (ii) critical and exact optical alignment and (iii) stable pump and probe beams.

5.5.1   Experimental set-up

The essential components for PTD technique are (1) a laser beam used as heat source called pump source used to heat the sample to produce a refractive index gradient (RIG). A He-Ne laser beam is used as a probe. A position sensitive detector with a lock-in technique is used for signal detection. A position sensitive detector (PSD) based on optical fibers was used in these experiments.

The schematic diagram of the experimental set-up used for PTD studies is shown in Figure 5.3.

The pump source used in these experiments is a continuous wave Ar ion laser (Liconix make, model no. 5302A), with a minimum power output of 3.3 mW for multiline multimode operation. 488 nm beam was selected for the studies. The set-up was initially standardised using 488 nm radiation.

The essential requirements for the probe beam source are good intensity and pointing.[23-26] The probe laser used for the PTD measurements is a He-Ne laser (632 nm radiation, 5 mW, Spectra Physics). The probe beam diameter should be less than the pump beam spot size. This was achieved by passing the probe beam through a pin-hole.

Light beam chopper, Ithaco model 230 with a chopping frequency of 3 Hz to 20 kHz was used for the modulation of laser beam.

The PSD was capable of precisely measuring the deflection suffered by a laser beam while passing through optically inhomogeneous regions in a medium. The sample, probe laser and PSD were mounted on XYZ translators.
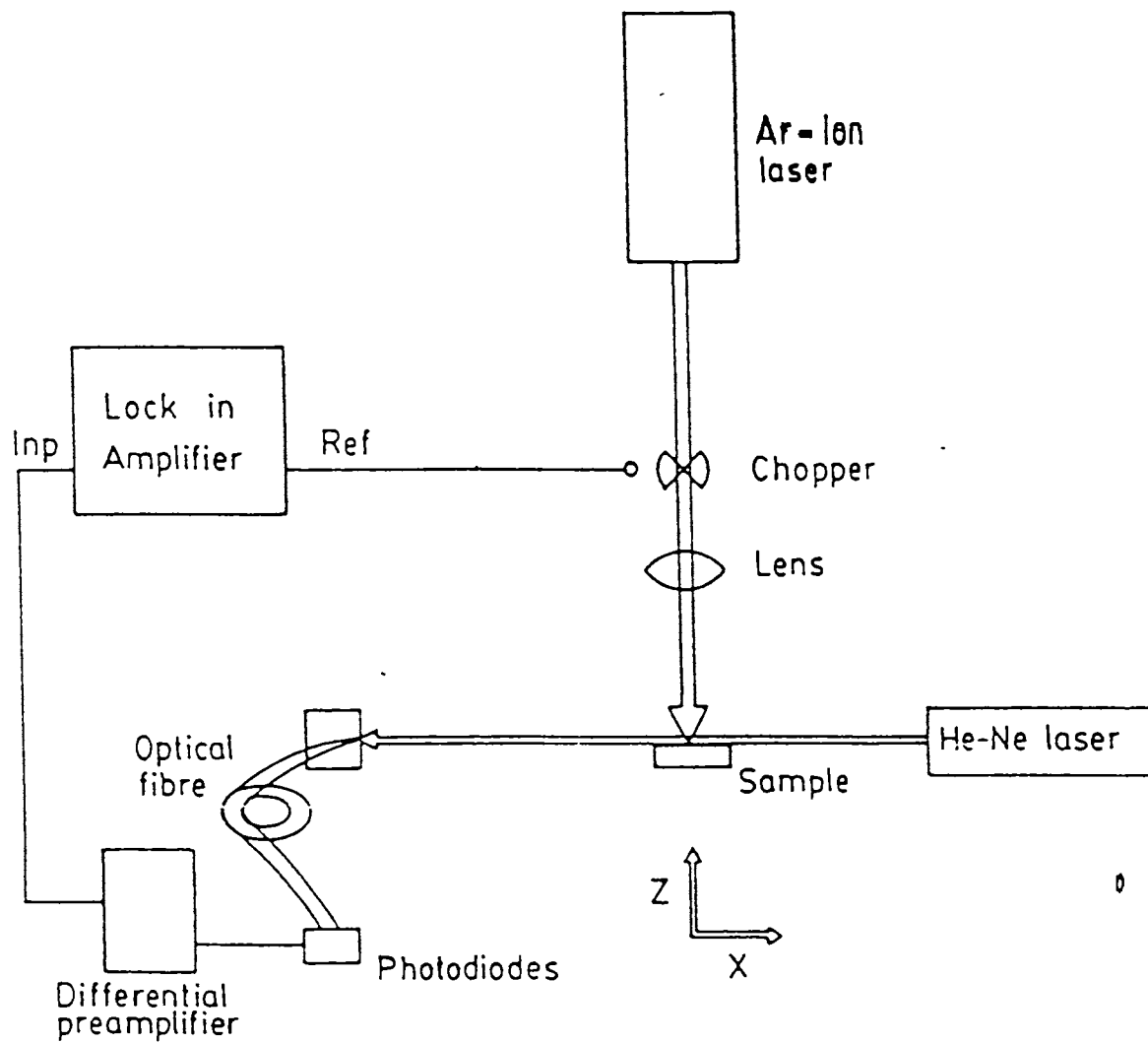
108

Fig.5.3   Schematic diagram of the experimental set-up used for PTD

studies

The signal output from the differential preamplifier was processed using a lock-in-amplifier (EG&G PARC 5208) which has an "auto setting" range, making possible the simultaneous and accurate measurements of phase and amplitude. The reference signal was taken from the electronics of the mechanical chopper.

5.6 RESULTS AND DISCUSSION

5.6.1 Evaluation of thermal diffusivity by PTD technique

The probe beam was adjusted to graze through the sample surface at a finite height (h) and the in-phase component of the deflection signal was measured at different positions (x) of the probe beam across the pump beam spot on the sample surface. The plot of phase shift vs x, shows a zero crossing on either side of the central zero at which the signal changes in phase by 180°. The typical plot of x vs phase shift for europium diphthalocyanine at two different chopping frequencies are given in the Figure 5.4.

The zero crossing points corresponds to points that are shifted in phase by $\pm 90^{\circ}$ relative to the central position. The thermal wavelength as a function of frequency is obtained from these points. Thus thermal wavelength at different frequencies were determined from the phase shift versus x plot. The temperature distribution of
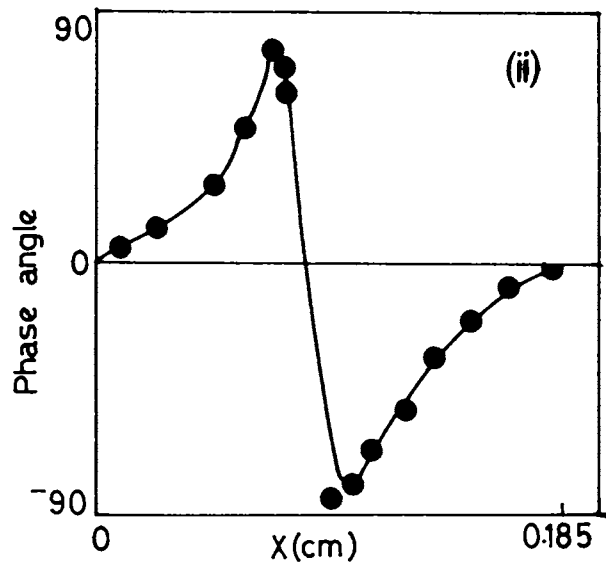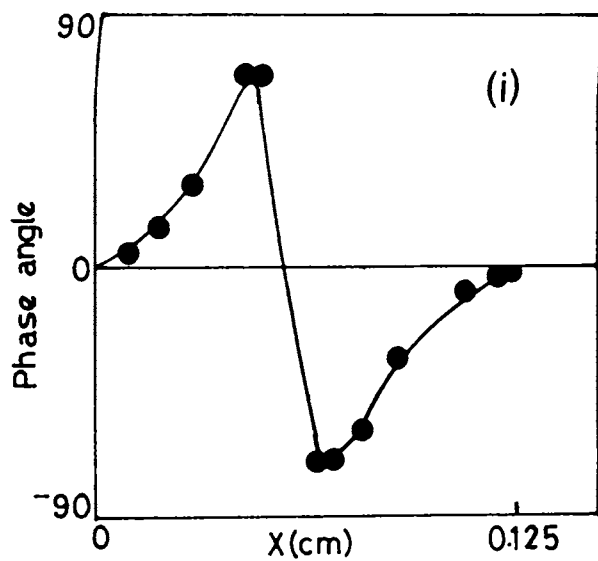
Fig.5.4   Plot   of   x   versus   phase   shift   for   europium
diphthalocyanine at two chopping frequencies.

(i)   172 Hz   (ii)   39 Hz

air very close to the sample surface can be taken as the temperature distribution of the sample surface since $\Delta T_s > \Delta T_g$ and the heat capacity of air is very small compared to that of solids. Thermal wavelength can be determined from the distance of separation between points of $\pm 90^{\circ}$ phase shift. The thermal diffusivity is obtained from the slope of the plot of thermal wavelength vs the reciprocal of the square root of the frequency.

According to Kuo et al,[27] the distance x_o is given by the expression,

$$x_o = d + (\gamma \pi \alpha / f)^{1/2} ,$$

where d is the intercept which is of the order of pump beam diameter and f is the chopping frequency. The slope of x_o vs $f^{-1/2}$ plot is $(\gamma \pi \alpha)^{1/2}$ where γ is a parameter which depends on the bulk thermo-optical properties of the sample. $\gamma = 1$ for optically transparent samples and $\gamma = 1.44$ for optically opaque samples. Thus the thermal diffusivity α can be determined from this plot.

The experimental set-up was standardised by determining the thermal diffusivity of copper (1.149 $cm^2 s^{-1}$) The value of thermal diffusivity obtained was in agreement with the reported value.[28]

During the experimental measurements, the low frequency region was given more importance in determining the slope of the plot

because the probe beam height is small when compared to the thermal wavelength in air. The thermal wavelength increases with decreasing frequency, decreasing the effective probe beam height.

The in-phase component of the deflection signal was measured at different positions (x) of the probe beam across the pump beam spot on the surface of H_2Nc, VONc, ZnNc, $Eu(Nc)_2$, and $Eu(Pc)_2$ samples for different frequencies. The phase angle was plotted as a function of x and x_0 was determined from this plot for each of the frequencies as shown in Figure 5.4.

The plot of x_0 (which is the distance between the zero crossing on either side of the central zero of a x vs phase shift graph) versus the reciprocal of the square root of frequency for different samples are given in Figures 5.5 to 5.7. The thermal diffusivity values obtained are presented in Table 5.1.

Thermal diffusivity is related to thermal conductivity by the relationship

$$\alpha = \frac{k}{\rho C}$$

where α is the thermal diffusivity, k is the thermal conductivity, ρ is the density and C is the specific heat capacity.

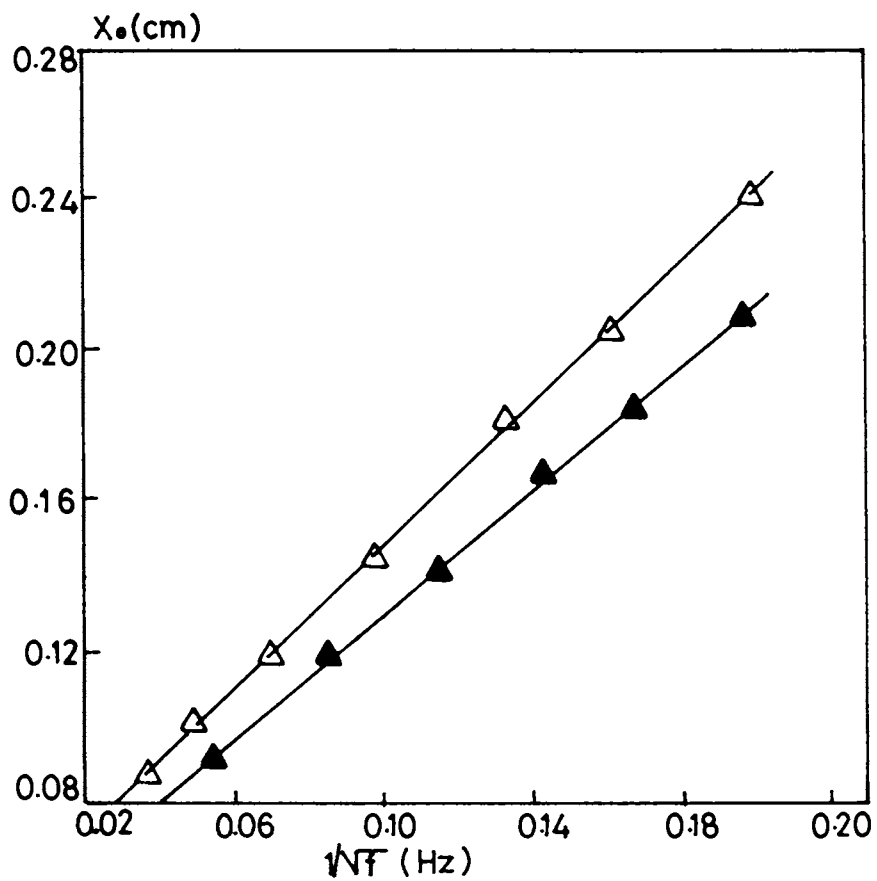Fig.5.5   The plot of x_0 versus reciprocal of sqaure root of

frequency for

VONc (—◁——◁—) and Eu(Nc)$_2$ (—◀——◀—).
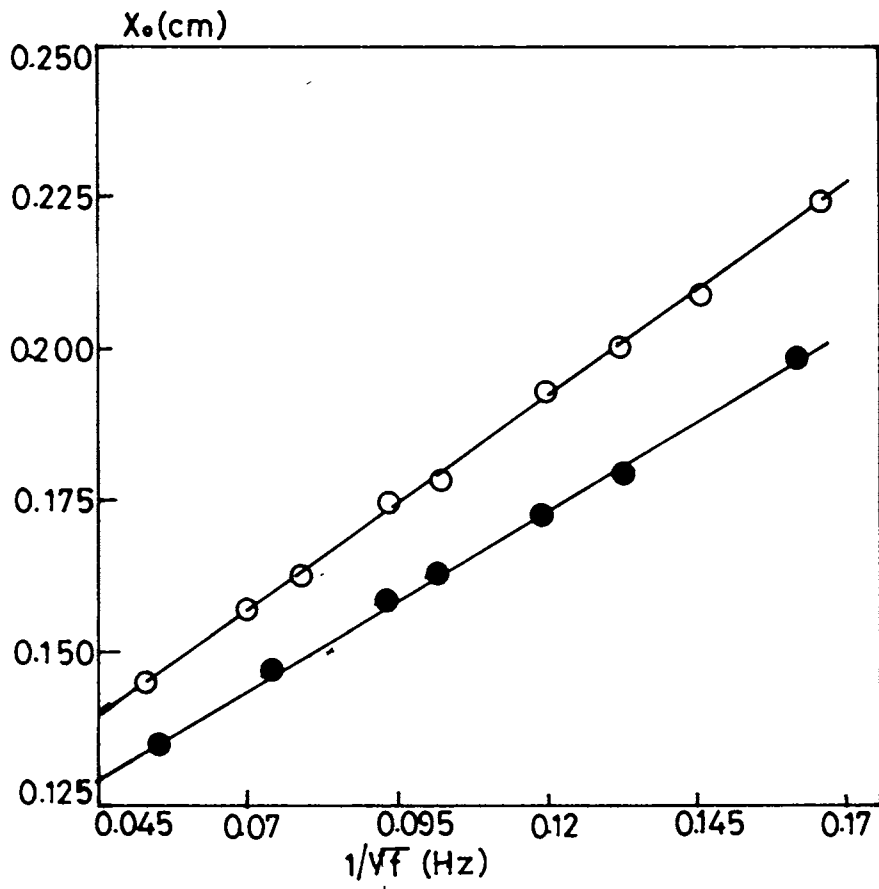
114

Fig.5.6   The plot of x_0 versus reciprocal of sqaure root of
frequency for

H_2Nc (—O——O—)   ZnNc   (—●——●—).

115
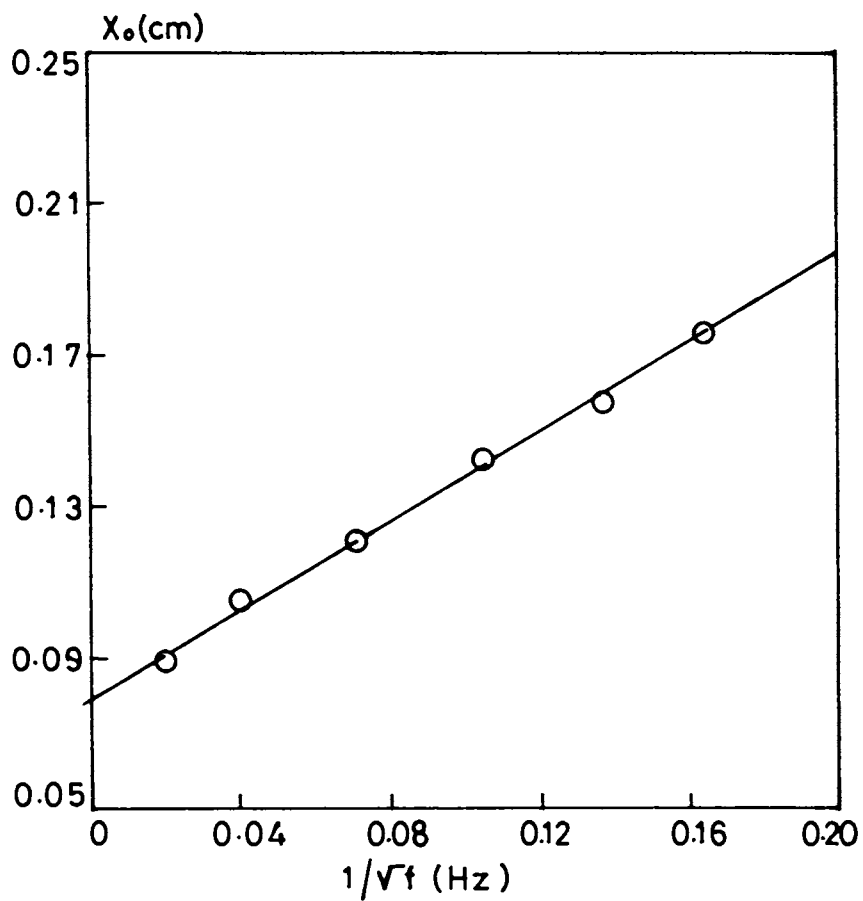
Fig.5.7   The plot of x_0 versus reciprocal of sqaure root of frequency for

Eu(Pc)$_2$ ($-\!O\!-\!\!-\!\!-\!O\!-$).

116

Table 5.1   Comparison of the thermal diffusivity values obtained
by PTD method and PA method

Samples	Thermal diffusivity by PTD method (cm^2s^{-1})	Thermal diffusivity by PA method (cm^2s^{-1})
ZnNc	0.11	0.10
VONc	0.29	0.26
H_2Nc	0.15	0.13
Eu(Nc)$_2$	0.22	0.20
Eu(Pc)$_2$	0.13	0.12

Since the central metal atom changes in different naphthalocyanines, the molecular arrangement of the material changes. Hence density and specific heat capacity of naphthalocyanines are different for differnt samples, thus changing the thermal diffusivity values.

In optical data recording (ODR), the information is stored,

117

usually in digital form, by using a modulated laser beam to induce a physical or chemical change in a recording medium. In ODR, the information is stored into the recording media in the form of grooves and pits using a diode laser. The information pieces were read from the character of the pits or grooves using semiconductor lasers. For these reasons the thermal parameters like thermal diffusivity of the recording medium are important considerations for selecting materials for ODR applications.

Organic materials have a number of advantages over inorganic materials for ODR applications. They are less prone to degradation caused by air and moisture. The zinc and vanadyl naphthalocyanines are recently reported as strong candidates for ODR.[29-31] Thermal diffusivity values of these materials are not reported in the literature. Hence the values reported herein will be useful in deciding its applicability relative to other materials.

REFERENCES

1. Yanagi, H.; Kouzeki, T.; Ashida, M.; Noguchi, T.;Manivannan, A.;Hashimoto, K.; Fujishima, A. *J. Appl. Phys.* 1992, 71(10), 5146.

2. Mc Donald, F.A.; Westel, G.C. Jr. *Physical Accoustics,* 18 WP Mason and Thussatin, R.N, (Ed), Academic Press, New York, 1986.

3. Andrew, C. Tam, A.C. Conference digest and technical abstracts, 7th International topical meeting on photoaccoustics and photothermal photothermal phenomina, 114, 1991.

4. Kuo, P.K.; Sendler, E.D.; Favro, L.D.; Thomas, R.L. *Can. J. Phys.*, 1986, 64, 1168.

5. Salazar, A.; Sanchez-Lavega, A.; Fernandez, J.; *J. Appl. Phys.*, 1989, 65, 4150.

6. Salazar, A.; Sanchez-Lavega, A.; Fernandez, J.; *J. Appl. Phys.*, 1991, 69, 1216.

7. Rosencwaig, A.; Gersho, A.; *J. Appl. Phys.* 1976, 47, 64.

8. Suber, G.; Bestolotti, M.; Sibillia, C.; Ferrasi, A.; Ricciardiello, F.G. *J. Therm. Anal.* 1987, 32, 1039.

9. Suber, G.; Bestalotti, M.; Sibillia, C.; Ferrari, A.; *Appl. Opt.* 1988, 27, 1807.

10. Inglehart, L.J.; Thomas, R.L. "Photothermal investigation of solids and fluids", Sell, J.A (Ed.), Academic Press, New York, 1988.

11. Kuo, P.K.; Lin, M.J.; Reys, C.B.; Favro, L.D.; Thomas, R.L.; Kim, D.S.; Zhang, S.Y.; Ingle Hast, L.J.; Fourmier, D,; Becara, A.C.; Jacoubi, N. *Can. J. Phys.*, 1986, 64, 1165.

12. Thomas, R. L.; Inglehast, L. J.; Lin, M. J.; Favro, L. D.; Kuo, P.K. Progs. Quant. Nondestr. Eval., Thompson, D. O.; Chiment, D.E. (Eds.), Plenum, New York, Vol. 4B, 1985, 859.

13. Rantala, J.; Acta Polytechnica Scandinavia, *Appl. Phys. Series,* No. 186, Helsinki, 1993.

14. Retala, J.; Wei, L.; Kuo, P. K.; Jassinen, J.; Luukkala, M.; Thomas, R.L.; *J. Appl. Phys.*, 1993, 73, 2714.

15. Hadj-Sahsaui, A.; Louis, J.; Mangeot, B.; Pesetti, P.; Billard, *J. Liq. Cryst.*, 1989, 5, 579.

16. Hadj-Sahsaui, A.; Louis, J.; Mangeot, B.; Pesetti, P.; Billard, P. *Phys. Rev. A.*, 1991, 44, 5080.

17. Rajasree, K.; Vidyalal, V.; Radhakrishnan, P.; Nampoori, V. P. N.; Vallabhan, C.P.G.; George, K.C. (To be published in *Liquid Crystals).*

18. Tsui, K.C.; Func, P.C.W.; Tam, H.L.; Walker, G.O. *J. Phys. Chem. Solids,* 1991, 52, 579.

19. Rajasree, K.; Vidyalal, V.; Radhakrishnan, P.; Nampoori, V.P.N.; Vallabhan, C.P.G.; Thomas, J.; Sinasankara Pillai, V.N. (To be published).

20. Bestolotti, M.; Monteneso, A.; Gnappi, G.; Liakhou, G.; Fazio, E.; Sibillia, C.; Schisone. L.; Vigoselli, A. *Mat. Sci. and Eng.*, 1991, B9, 433.

21. Bertolott, M.; Ferrari, A.; Fazio, E.; Livoti, R.; Sibillia, C.; Chumack, C.; Liakhou, G.; Popescu, C. *Mat. sci. Eng.,* 1991, B9, 459.

22. Bestolotti, M.; Fazio, E.; Fessri, A.; Liakhou, G.; Gnappi, G.; Monteneso, A.; Rossi, C.; Gizimin. *Mat. Sci. and Eng.*, 1990, B5, 143.

120

23. Aamodt, L.C.; Murphy, J.C. *J. Appl. Phys.* 1981, 52, 4903.36.

24 Lasalle, L.E.; Lepoutre, F.; Roger, J.P. *J. Appl. Phys.* 1988, 64, 1.

25. Mc Donald, F.A.; Wetsel, G.C. Jr.; Jamieson, J.E. *Can. J. Phys.* 1986, 64, 1265.

26. Spear, J.D.; Russo, R.E.; Silva, R.J. *Appl. Opt.* 1990, 29, 4225.

27. Kuo, P.K.; Favro, L.D.; Thomas, R.L.; *"Photothermal investigations of solids and fluids"*, Sell, J.A. (Ed.) Academic Press, New York, 1988.

28. Weasat, R.C. (Ed.),*"Handbook of Chemistry and Physics"*, 61 Ed.,(Boca R Raton : Chemical Rubber Company), 1980.

29. Yanagi, H.; Ashida, M.; Elbe, J.; Wohrle, D. *J. Phys. Chem.* 1990, 94,7056.

30. Yanagi, H.; Kouzeki, T.; Ashida, M.; Noguchi, T.;Manivannan, A.;Hashimoto, K.; Fujishima, A. *J. Appl. Phys.* 1992, 71(10), 51.46.

31. Bergbreiter, D.E.; Martius, C.R.(Eds.) *"Functional Polymers"*, Plenum Press, New York.

This study was targeted to evaluate the electrical and photothermal characteristics of five compounds namely metal free naphthalocyanine [H_2Nc], vanadyl naphthalocyanine [VONc], zinc naphthalocyanine [ZnNc], europium dinaphthalocyanine [Eu(Nc]$_2$, and europium diphthalocyanine [Eu(Pc)$_2$, and their iodine doped forms. Doping using iodine under controlled conditions give compounds with stoichiometry as given in Table 6.1.

Table 6.1   Stoichiometry of iodine doped compounds

Compound	stoichiometric formula of pristine compound	stoichiometry of doped form
Metal free naphthalocyanine	$C_{48}H_{26}N_8$	$C_{48}H_{26}N_8I_{0.11}$
Vanadyl naphthalocyanine	$VOC_{48}H_{24}N_8$	$VOC_{48}H_{24}N_8I_{0.12}$
Zinc naphthalocyanine	$ZnC_{48}H_{24}N_8$	$ZnC_{48}H_{24}N_8I_{0.12}$
Europium dinaphthalocynine	$EuC_{96}H_{49}N_{16}$	$EuC_{96}H_{49}N_{16}I_{0.02}$
Europium diphthalocyanine	$EuC_{64}H_{33}N_{16}$	$EuC_{64}H_{32}N_{16}I_{0.02}$

A higher uptake of iodine is observed for metal naphthalocyanine. For europium dinaphthalocyanine and europium diphthalocyanine, iodine uptake is much lower.

Electrical conductivity is one of the most important parameters for molecular semiconductors used in electrical transduction. Also an understanding of the mechanism of electrical conduction is necessary to predict the changes that are likely to occur under a given set of conditions like temperature and doping. The electrical properties were measured on pristine and iodine doped samples.

The dc conductivities of H_2Nc, VONc, and $Eu(Pc)_2$ are virtually independent of temperature in the low temperature range. At higher temperatures, conductivity increases with temperature. Such an increase in conductivity and a change in activation energy above certain temperature is indicative of thermally activated process taking place in these materials. The process may be a lattice expansion, thermally activated release of charge carriers from trapped states or any other mechanism that may aid this process. In all the three cases, iodine-doped forms have enhanced conductivity. The shape of the Arrhenius plot changes especially in the case of VONc. The sharp bend in the Arrhenius plots

disappears and the plots have a low curvature. This indicates that more or less the same mechanism of conduction exists throughout the temperature range. In the case of $Eu(Pc)_2$ and $Eu(Pc)_2I$, the change in conduction mechanism is smooth. Such a plot is usually indicative of the existence of a mixed conduction mechanism in the transition region.

ZnNc and $Eu(Nc)_2$ show considerable dependence on conductivity with temperature. Both the compounds lack a sharp bend in the Arrhenius plot. However, in the higher temperature range, the slope is slightly larger. ZnNcI and $Eu(Nc)_2I$ show a higher conductivity than their pristine forms.

The ac conductivity measurement as a function of frequency as well as temperature is a diagnostic tool to evaluate the conduction mechanism in quasi-one-dimensional molecular systems. The σ_{ac} of H_2Nc, VONc, and $Eu(Nc)_2$ depend both on temperature and frequency. Such a behavior is typical of a mechanism involving hopping in a manifold of states. In the iodine-doped forms the conductivity is enhanced, but the temperature and frequency dependence follows the same pattern as the corresponding pristine materials.

ZnNc shows some unique features. At low frequencies, the temperature dependence of ac conductivity shows a broad peak which

125

is characteristic of a relaxation phenomenon associated with macromolecular chains. This broad peak disappears in the iodine-doped form. In the three frequencies selected the conductivities show a pattern dependent on frequency as well as temperature. The broad peak is rather ill defined. However iodine-doped form show conductivity which is fairly independent of temperature at the frequencies measured. Thus the material is equivalent to metal-insulator composite.

Metal naphthalocyanines are promising materials as material media for optical recording by pit formation. This is especially so when infrared lasers are used due to the better definition of patterns that can be achieved. The thermal diffusivity of the medium decides the suitability in this application. Hence the evaluation of the thermal diffusivity of the materials were carried out using photoacoustic and photothermal deflection techniques. The results are summarised in Table 6.2.

Table 6.2 Thermal diffusivity values obtained by photoacoustic (PA) and photothermal deflection (PTD) methods.

Sample	Thermal Diffusivity (cm^2 s^{-1})	
	By PA Method	By PTD Method
H_2Nc	0.13	0.15
H_2NcI	0.17	
VONc	0.26	0.29
VONcI	0.29	
ZnNc	0.10	0.11
ZnNcI	0.15	
$Eu(Nc)_2$	0.20	0.22
$Eu(Nc)_2I$	0.23	
$Eu(Pc)_2$	0.12	0.13
$Eu(Pc)_2I$	0.14	

In pristine naphthalocyanine, the thermal diffusivity is very much enhanced upon doping. Such an enhancement of thermal diffusivity is observed with $Eu(Nc)_2$, $Eu(Pc)_2$ and their iodine-doped forms. But the magnitude of increase is less in these

127

materials. Of the metal naphthalocyanines studied ZnNc has the lowest thermal diffusivity, but a 50% increase is observed upon doping. Compared to $Eu(Pc)_2$, $Eu(Nc)_2$ has a higher thermal diffusivity. Of the materials studied VONc has the highest thermal diffusivity. These results indicate that when we are searching for a material of low thermal conductivity, the choice falls on ZnNc or H_2Nc. On the other hand, if we are searching for one with a large thermal diffusivity, the choice is VONc or $Eu(Nc)_2$. In general, the iodine-doped form have a higher thermal diffusivity.

The measurement of thermal diffusivity by photothermal deflection technique gives values which are in good agreement with those obtained by photoacoustic technique and thus are mutually supportive. The thermal diffusivity of these materials have not been reported earlier. The values reported herein are helpful in making a choice of the suitable material for optical data recording.

This work has revealed some novel information on the conduction mechanism in five macrocyclic compounds and their iodine-doped forms. Also useful data on the thermal diffusivity of the target compounds have been obtained by optical techniques. This is a modest contribution to the material science aspect of naphthalocyanines and phthalocyanines.

The work presented in this dissertation has been published/communicated in the following forms:

1. "Electrical conductivity and thermal diffusivity of zinc naphthalocyanines."

   Jayan Thomas, V.N.Sivasankara Pillai, Edwin Xavier and C.P.G.Vallabhan (accepted for publication in Mat. Sc. Lett.)

2. "Electrical conductivity and thermal diffusivity of vanadyl naphthalocyanine."

   Jayan Thomas, V.N.Sivasankara Pillai, Edwin Xavier and C.P.G.Vallabhan (communicated to Chem. Phys. Lett.)

Cognate Publications

1. "Thermal diffusivity of metal phthalocyanines determined by photothermal deflection technique"

   K. Rajasree; V. Vidyalal; P. Radhakrishnan; V.P.N. Nampoori; C.P.G. Vallabhan; Jayan Thomas and V.N. Sivasankara Pillai (communicated to Chem. Phys. Lett.)

2. "Inhibition of corrosion of aluminium in hydrochloric acid by cobalt tetrasulphophthalocyanines."

V.N.Sivasankara Pillai; Jayan Thomas and P.S. Harikumar

Ind. J. Chem. Technol. 1995, 2, 99.

3. "Electron-transfer mediation by RF plasma treated iron, nickel, and zinc phthalocyanines".

P.S. Harikumar; Jayan Thomas and V.N. Sivasankara Pillai

(acepted for publication in Bull. Electrochem.)

4. "Photoacoustic measurement of thermal diffusivity in metal phthalocyanines."

Edwin Xavier; C.P.G. Vallabhan; Jayan Thomas and V.N. Sivasankara Pillai (communicated to J. Phys. Chem.)

Symposium presentations:

1. "Thermal diffusivity measurements in phthalocyanines by photothermal deflection technique". Symposium on Molecular Spectroscopy and Lasers, Nov. 26-28, 1994, Varanasi, INDIA.

K. Rajasree; V. Vidyalal; P. Radhakrishnan; V.P.N.Nampoori; C.P.G. Vallabhan; Jayan Thomas and V.N. Sivasankara Pillai.

2. "Use of photothermal deflection technique for the determination of thermal diffusivity of metal phthalocyanines."

National Laser Symposium, Feb. 10-14, 1995, Dehradun, INDIA.

K. Rajasree; V. Vidyalal; P. Radhakrishnan; V.P.N.Nampoori; C.P.G. Vallabhan; Jayan Thomas and V.N. Sivasankara Pillai.

3. "Thermal diffusivity measurement of certain metal phthalocyanines using photoacoustic technique."

National Laser Symposium, Feb. 10-14, 1995, Dehradun, INDIA.

Edwin Xavier; C.P.G. Vallabhan; Jayan Thomas and V.N. Sivasankara Pillai.

4. "Thermal diffusivity measurement of europium diphthalocyanine using laser photoacoustic technique."

National Symposium on Current Trends in Coordination Chemistry, March 23-25, 1995, Cochin, INDIA.

Jayan Thomas; V.N. Sivasankara Pillai; Edwin Xavier and C.P.G. Vallabhan.